Technical Assistance Consultant's Report

Project No: 42384-012
November 2020

Knowledge and Innovation Support for ADB's Water Financing Program

Remote Sensing Based Water Productivity Assessment in four irrigation schemes, Cambodia

Prepared by

International Water Management Institute

For Asian Development Bank

ASIAN DEVELOPMENT BANK

Remote Sensing Based Water Productivity Assessment in four irrigation schemes, Cambodia

FINAL REPORT

IWMI International Water Management Institute

CGIAR RESEARCH PROGRAM ON Water, Land and Ecosystems

ADB

Project final report submitted to the Asian Development Bank under the program for Expanding support to Water Accounting in River Basins and Water Productivity in Irrigation Schemes. The designations employed and the presentation of material in this information product do not imply the expression of any opinion whatsoever on the part of the Asian Development Bank (ADB) or the International Water Management Institute (IWMI) concerning the legal or development status of any country, territory, city or area or of its authorities, or concerning the delimitation of its frontiers or boundaries. The mention of specific companies or products of manufacturers, whether or not these have been patented, does not imply that these have been endorsed or recommended by ADB or IWMI in preference to others of a similar nature that are not mentioned. The views expressed in this information product are those of the author(s) and do not necessarily reflect the views or policies of ADB or IWMI.

Citation: Matheswaran, K., and Rebelo, L-M., 2020. Remote Sensing Based Water Productivity Assessment in four irrigation schemes, Cambodia. Final Project Report. IWMI, Colombo, Sri Lanka

Cover image: Irrigated rice fields in Southeast Asia, Jim Holmes / IWMI

EXPANDING SUPPORT TO WATER ACCOUNTING IN RIVER BASINS AND WATER PRODUCTIVITY IN IRRIGATION SCHEMES

Project final report:

Remote Sensing Based Water Productivity Assessment in four irrigation schemes, Cambodia

PREPARED FOR THE
ASIAN DEVELOPMENT BANK
BY

The International Water Management Institute

November 2020

Table of Contents

List of Figures

List of Tables

List of abbreviations

ADB	Asian Development Bank
AGBP	Above Ground Biomass Production
C15IS	Canal 15 Irrigation Scheme
CWP	Crop Water Productivity
CWSI	Crop Water Stress Index
DSS	Decision Support System
ET_a	Actual Evapotranspiration
FAO	Food and Agriculture Organization
GEE	Google Earth Engine
GLDAS	Global Land Data Assimilation System
HI	Harvest Index
IAIP	Irrigated Agriculture Improvement Project
IHE Delft	IHE Delft Institute for Water Education
IWMI	International Water Management Institute
KPIS	Kamping Pouy Irrigation Scheme
MCM	Million Cubic Meters
MODIS	Moderate Resolution Imaging Spectroradiometer
NASA	National Aeronautics and Space Administration
NDVI	Normalized difference vegetation index
PPIS	Prek Po Irrigation Scheme
PySEBAL	Python implementation of SEBAL
RWD	Relative Water Deficit
SCIS	Stung Chinit Irrigation Scheme
SRTM	Shuttle Radar Topography Mission
TA	Technical Assistance
WP	Water Productivity
USGS	United States Geological Survey

I. BACKGROUND

1. The ADB is committed under its Water Operational Plan 2011-2020 to undertake expanded and enhanced analytical work to enable its developing member countries to secure a deeper and sharper understanding of water issues and solutions. IHE Delft, in collaboration with IWMI and FAO, will support ADB in achieving this objective.

2. The activities proposed under the current study build on the work previously undertaken by IHE Delft and IWMI in cooperation with the Asian Development Bank (ADB) to assess crop water productivity and to assess water resource status in selected countries in Asia.

3. Through the current study, IHE Delft in partnership with its subcontracted partner, IWMI, will support (a) ADB's lending and non-lending assistance in the water sector, and (b) the design of irrigation projects at an early stage at selected candidate projects.

4. IHE Delft and IWMI and aim to support ADB's lending and non-lending assistance in the water sector by creating (i) comprehensive, (ii) comprehensible, and (iii) accessible information on available water resources and their current uses in major river basins. IHE Delft and IWMI aim to support the design of, or investments in irrigation schemes at project start by (i) providing baseline data for parameters related to land and water productivity, and (ii) identifying suitable interventions.

5. Assistance is being provided to projects in seven target countries. The nature of the support provided in each is determined through close consultation with ADB Project Officers and tailored to the project requirements. In some locations, this may take the form of water accounting assessments to characterize water use and availability, while in others emphasis may be placed on water productivity (either crop or biomass water productivity), or on irrigation performance assessments, to target investments.

6. This project aimed to contribute to sustainable development in Asia's irrigation sector, and to create more value from scarce water resources. Cambodia is one of the five countries where advanced technologies to measure WP from satellite data has been introduced. This Final Project Report details the activities undertaken in Cambodia.

II. SCOPE OF SERVICES

7. The activities reported here are intended to support The Irrigated Agriculture Improvement Project (IAIP). The IAIP will assist the Government of Cambodia to modernize and improve climate and disaster resilience of four irrigation systems in Battambang, Kampong Cham, Kampong Thom, and Takeo provinces to supply water to 43,500 hectares. Civil works are proposed under the subproject to achieve this, including rehabilitation of canals to ensure water delivery

8. The four selected irrigation schemes, namely Kamping Puoy (KPIS), Stung Chinit (SCIS), Prek Po (PPIS), and Canal 15 (C15IS) located in the Battambang, Kampong Cham, Kampong Thom, and Takeo provinces in Cambodia are the Subprojects of the IAIP. These

schemes were proposed by the Ministry of Water Resources and Meteorology (MOWRAM) of the Royal Government of Cambodia (RGC) for loan funding by the Asian Development Bank (ADB).

9. In discussion with ADB, IWMI has agreed to undertake a water productivity assessment for the four Subprojects. This will focus on the generation and analysis of Actual Evapotranspiration (ET_a) estimates from remote sensing, Relative Water Deficits (RWD), and Above Ground Biomass Production (AGBP) for the irrigation schemes. The agreed deliverables are:

a) Evapotranspiration maps at 30 meter spatial resolution
b) Biomass production maps at 30 meter spatial resolution
c) Crop (rice) water productivity maps at 30 meter spatial resolution
d) A final report describing the results and interpretations of the outputs.

10. The assessment was carried out for three irrigation seasons which start in December and finish in April for the period 2016/2017 to 2018/2019. Paddy rice is the main crop cultivated in both the irrigated and rainfed seasons.

III. IMPLEMENTATION OF ACTIVITIES

A. Study area description

11. All four irrigation schemes are located within the Mekong river basin. The KPIS is in the Tonle Sap river basin (a sub-basin of Mekong), while the other three are located along the main Mekong river (*Figure 1*). Located in the tropical climate, the summer season starts in March and extends up to May followed by the monsoon season from June to October, while the winter season is from November to February. Paddy is the dominant crop in all four irrigation schemes in both wet (rainfed) season and dry (irrigation) season. A two-rice cropping system is practiced predominantly in the command area of all four irrigation schemes. During the monsoon season, traditional long maturity paddy rice is planted in the middle of June and harvested in November. During the dry season, an early maturity variety is planted in December and harvested in April. The reported rice yields of traditional and modern varieties within these three irrigation schemes range from 3.5–5 t/ha (IAIP, 2019a, b, and c). The generalized crop calendar (wet and dry season) for these four irrigation schemes is shown in *Figure 2*.

12. ***KPIS:*** The KPIS in Battambang province in northwestern Cambodia stretches for 35 km from west of Battambang Town to the Kamping Pouy reservoir (Figure 3a). The Battambang province is known as the “Rice Bowl” of Cambodia accounting for 12% of Cambodia’s rice production (MAFF, 2011). Two-rice cropping system is practiced predominantly in KPIS command area. Some farmers with access to supplementary water sources also practice three rice cropping system. The KPIS utilizes water from two tributaries of Tonle Sap sub-basin. The reservoir has a maximum storage capacity of 139 million cubic meters (MCM), from which 101 mcm is available for irrigation and the remaining for flood control (IAIP, 2019). Water availability in the reservoir is augmented by additional supply from the Mongkol Borey River through a 13.9 km link canal to fill the reservoir up during the monsoon season. The KPIS system serves 19,000 ha, from which 12,000 ha is the command

area of the Subproject (IAIP, 2019). The Subproject area is served by outlet no. 4 through a 9.8 km main canal and three secondary canals. The main canal provides water for the secondary canals that run through the network and carries water to different blocks within the KPIS. The KPIS command area is divided into seven irrigation blocks. Blocks A and B are served directly by the main canal and the rest of the area through three secondary canals. The Feasibility Study (IAIP, 2019) reports that the current infrastructure does not have adequate capacity to allow farmers at the tail end of the secondary canals to get enough water for irrigation. To mitigate the lack of water from the irrigation system, some farmers employ pumps to irrigate their fields.

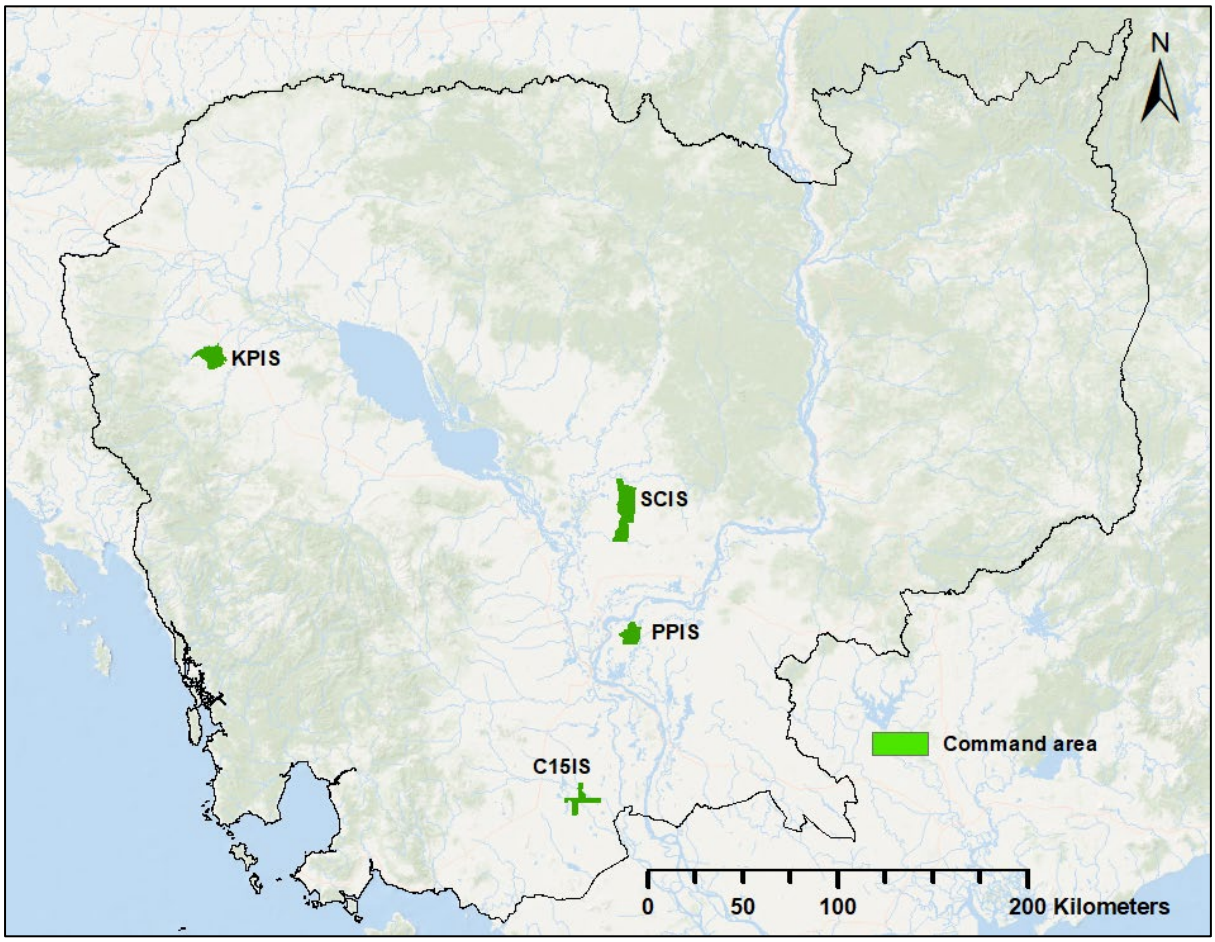

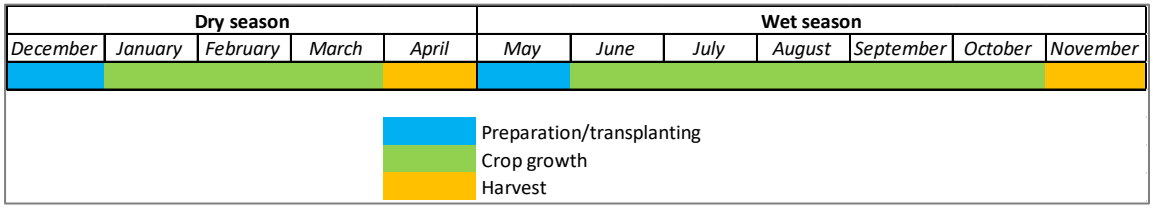

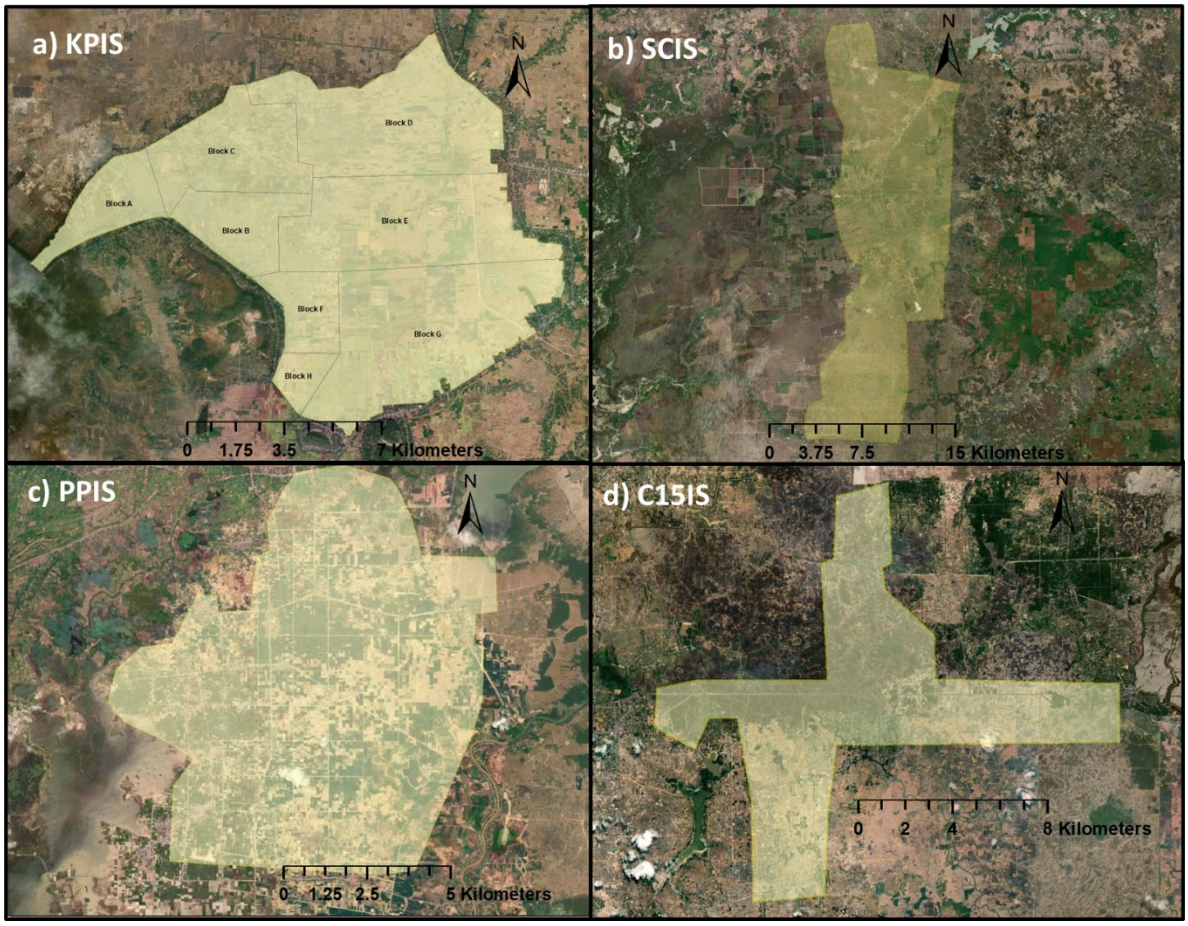

Figure 3: Command area of the a) KPIS, b) SCIS, c) PPIS and d) C15IS irrigation schemes

13. ***SCIS***: The SCIS Subproject includes 19,900 ha of command area served by the south main canal from Stung Chinit reservoir (Figure 3b) (IAIP, 2019a). The north main canal has a command area of 3,046 ha which also supplements the Taing Krasaing River irrigation system. The canal network originating from the south main canal is 37 km long and connects to around 76 km of secondary and tertiary canals. Most of the canal section is dilapidated because of poor maintenance; this undermines significantly the carrying capacity of the canal network. It should be noted that during the dry season cultivation is concentrated in farms along or close to the main canal owing to lack of water availability.

14. ***PPIS***: The PPIS system serves 8,000 ha of agricultural land in Kampong Cham province (Figure 3c) (IAIP, 2019b). The Mekong is the main source of water for the PPIS from which the water is lifted to a 13 km long main canal. In addition to the main canal, the PPIS irrigation network consists of 20 secondary canals and seven tertiary canals. PPIS has not been operational since 2015 due to reduced efficiency and high operating cost of the pumping system and poor conditions of the canal networks. Farmers in the PPIS undertake agricultural activities mainly during the rainfed season. Fields are irrigated by pumping accumulated rainwater into the canal network. Farmers employ supplementary irrigation with water supplied through natural ponds and shallow tube wells. The command area is mostly suitable for lowland rice cultivation. Depending on water availability in the canal as a result of rainfall, and access to other water sources, some farmers produce two to three rice crops per year.

15. ***C15IS***: The Subproject area of the C15IS system consists of 7,500 ha of command area (Figure 3d) (IAIP, 2019c). The main canal of C15IS is directly fed by the Bassac River and the water level fluctuates daily in response to the changes in river water level. The Subproject is served by the C15IS main canal, and two sub-systems consisting of Canal 87 and the Samput pumping system. The main canal and its secondary canal (called Canal 87) serve 6,500 ha of lowland area (1 to 3 m msl), while the Samput pumping system serves 1,000 ha of upland command area (5 to 10 m msl). The main canal, which runs east-west provides water for the secondary canal that runs through the network and carries water to different blocks within C15IS. The canals serving the command area of C15IS have gradually deteriorated due to lack of maintenance leading to low water flows in the dry season. Farms along the main canal have preferential water access compared to farms experiencing water shortages located far from the main canal. The inadequate capacity of current infrastructure does not allow farmers at the tail end of the secondary canals to get enough water for irrigation. Some farmers along the main canal opt for pumping canal water or shallow groundwater to supplement their irrigation needs during water scarce situations. Since the command area is a part of the Mekong floodplain, it is generally flooded from June to October; single or sometimes double cropping of flood recession rice is therefore common.

B. Input Data

16. For setting up the PySEBAL model, meteorological data at the time of satellite data acquisition (instantaneous) and 24-hour average representing the day of acquisition are required. The meteorological data required are listed in Table 1. These data were extracted for the SCIS, PPIS and C15IS from NASA Global Land Data Assimilation System (GLDAS v2.1) which is an assimilated global data product from satellite and ground-based observations. GLDAS data is offered at 0.25^{o} spatial resolution at 3 hours interval. For topography and elevation, 30 m NASA's Shuttle Radar Topography Mission (SRTM) data available through USGS Earth explorer was used. The PySEBAL model processes the extent of Landsat 8 imagery defined by the Digital Elevation Model (DEM) extent called processing unit which is shown in Figure 3.

Table 1 Meteorological data and its units used for the PySEBAL model

Parameter	**Symbols**	**Unit**
Downward shortwave radiation	SW_{down}	W/m^2
Wind speed	W_s	m/s
Air temperature	T_{air}	°C
Pressure	P	Mb
Relative humidity	Rh	%

17. The command area of KPIS is covered by a Landsat scene from path 127 and row 57, SCIS by a Landsat scene with path 128 and row 51 and the remaining two schemes are covered by Landsat scene with Path 128 and row 52 (Figure 4). A total of 167 Landsat 8 scenes between 01 September 2016 and 30 June 2019 were acquired through the USGS Earth explorer (https://earthexplorer.usgs.gov/) database, for the four irrigation schemes

covering three irrigation seasons. Dates of image acquisitions and corresponding cloud cover (%) for each irrigation scheme are provided in Table 2.

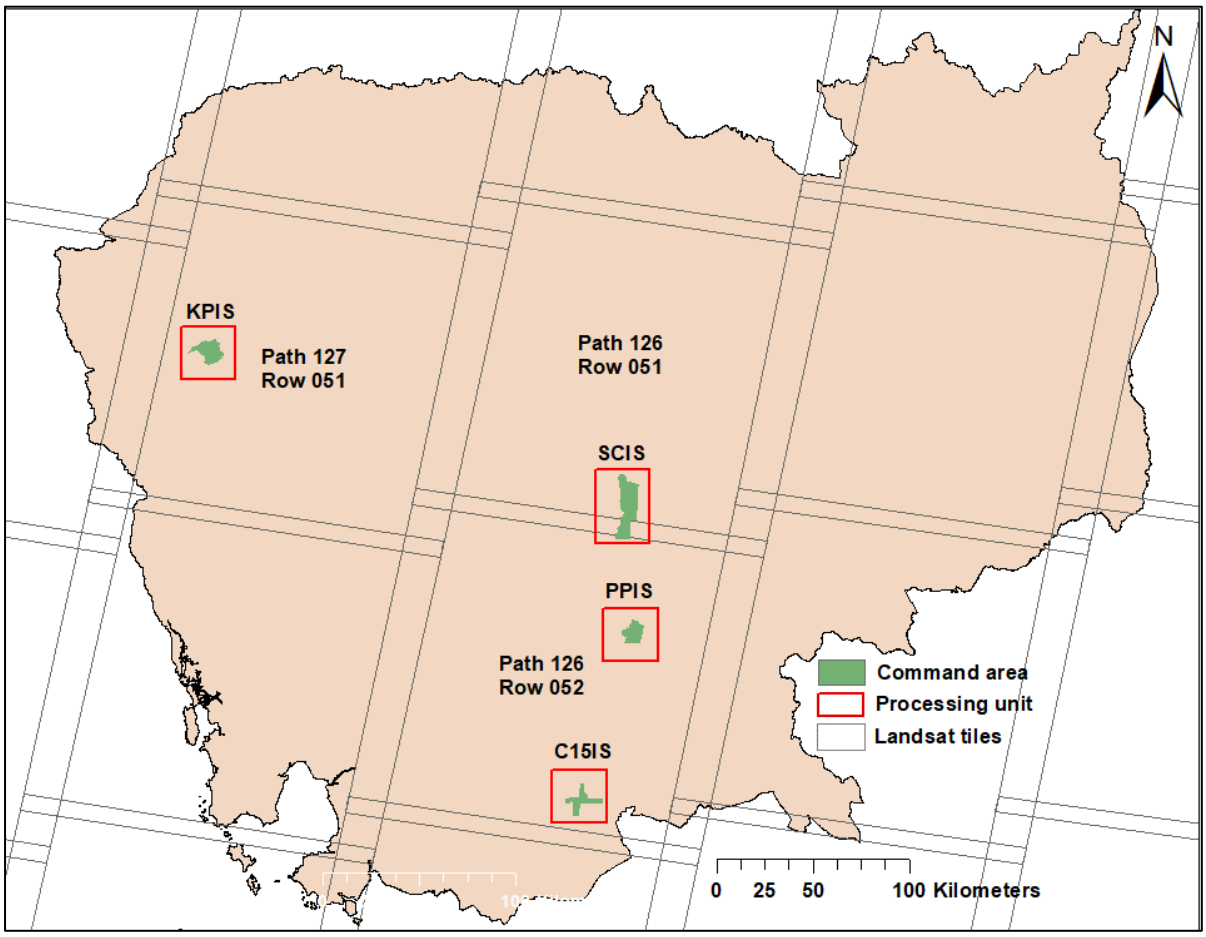

Figure 4: Landsat tiles and processing unit of PySEBAL model over the four selected irrigation schemes

18. Accuracy of remote sensing-based analysis is always dependent on the availability of cloud free images over the study period (Karimi and Bastiaanssen, 2015). Annex 1 shows the aggregated seasonal cloud cover in three irrigation schemes for 2016/2017, 2017/2018 and 2018/2019. The cloud cover map directly relates to the the quality of the estimated seasonal ET_a and AGBP maps presented in this report and are presented to help users in determining the suitability of the estimated values for different applications. Each pixel value in Annex 1 represents the percentage of time within a given season under cloud cover. For instance, a value of 60% indicates that the pixel is under cloud cover for 60 % of the obtained Landsat 8 scenes within a season. In addition, the robust spatial and temporal gapfilling methods used in this study help significantly with improving quality of the remote sensing estimates even when and where gaps in satellite data acquisitions exist.

Table 2 Landsat 8 image acquisition dates and cloud cover (CC %) for the four selected irrigation schemes

Scene	Date	CC (%)	Date	CC (%)	Date	CC (%)	Date	CC (%)		Date	CC (%)		Date	CC (%)	
	2016/2017	KPIS	2017/2018	KPIS	2018/2019	KPIS	2016/2017	SC	PP & C15	2017/2018	SC	PP & C15	2018/2019	SC	PP & C15
1	05-09-2016	71	08-09-2017	82	11-09-2018	30	14-09-2016	70	41	01-09-2017	35	16	04-09-2018	58	63
2	21-09-2016	99	24-09-2017	68	27-09-2018	8	30-09-2016	-	93	17-09-2017	59	56	20-09-2018	26	39
3	07-10-2016	74	10-10-2017	58	13-10-2018	37	16-10-2016	-	88	03-10-2017	-	58	06-10-2018	30	49
4	23-10-2016	47	26-10-2017	30	29-10-2018	25	01-11-2016	42	65	19-10-2017	63	-	22-10-2018	37	23
5	08-11-2016	66	11-11-2017	57	14-11-2018	58	17-11-2016	23	22	04-11-2017	98	90	07-11-2018	86	-
6	24-11-2016	42	27-11-2017	45	30-11-2018	25	03-12-2016	49	63	20-11-2017	89	-	23-11-2018	71	63
7	10-12-2016	46	13-12-2017	41	16-12-2018	22	19-12-2016	45	62	06-12-2017	2	-	09-12-2018	10	34
8	26-12-2016	27	29-12-2017	4	01-01-2019	11	04-01-2017	4	63	22-12-2017	18	1	25-12-2018	6	11
9	11-01-2017	37	14-01-2018	76	17-01-2019	2	20-01-2017	12	52	07-01-2018	67	49	10-01-2019	25	26
10	27-01-2017	2	15-02-2018	0	02-02-2019	7	05-02-2017	4	16	23-01-2018	40	46	26-01-2019	8	34
11	12-02-2017	2	03-03-2018	13	18-02-2019	21	09-03-2017	34	41	08-02-2018	4	72	11-02-2019	0	0
12	28-02-2017	0	19-03-2018	9	06-03-2019	1	25-03-2017	44	38	24-02-2018	33	16	27-02-2019	0	5
13	16-03-2017	42	04-04-2018	46	22-03-2019	1	10-04-2017	71	57	12-03-2018	0	14	15-03-2019	11	5
14	17-04-2017	29	20-04-2018	24	07-04-2019	27	26-04-2017	27	40	28-03-2018	70	5	31-03-2019	1	52
15	03-05-2017	38	06-05-2018	49	23-04-2019	47	12-05-2017	35	14	13-04-2018	20	25	16-04-2019	86	26
16	19-05-2017	80	22-05-2018	87	09-05-2019	96	28-05-2017	63	31	29-04-2018	-	32	02-05-2019	23	73
17	04-06-2017	26	07-06-2018	94	25-05-2019	11	13-06-2017	82	56	15-05-2018	20	92	18-05-2019	-	17
18	20-06-2017	12	23-06-2018	13	10-06-2019	40	29-06-2017	42	27	31-05-2018	89	50	03-06-2019	52	22
19					26-06-2019	40				16-06-2018	82	23	19-06-2019	50	29

C. Mapping Evapotranspiration and Above Ground Biomass

19. The acquired Landsat 8 data were pre-processed to create cloud masked Top Of Atmosphere (TOA) reflectance bands. The preprocessing included conversion from Digital Number (DN) to TOA reflectance, cloud removal using the Quality Assessment (QA) band provided along with the data and mosaicking the same path tiles. All the satellite data preprocessing is done inside PySEBAL. The preprocessing of the meteorological data includes the following steps: i) extract the variable and clip to the study area, iii) convert the units of air temperature from Kelvin to °C, pressure from Pascal (Pa) to Millibar (mb), and specific humidity in kg/kg to the relative humidity in %, and iv) extract instantaneous and aggregate daily average meteorological variables from the three-hourly data. The instantaneous data corresponding to the Landsat acquisition time (10:30 A.M local time) was estimated by averaging the 6 hour and 9 hour outputs from GLDAS, and all of the images for a single day were averaged to estimate 24 hours representing the day of the Landsat acquisition.

20. The entire processing chain was performed using multiple open-source libraries, for handling multi-core jobs, processing satellite data, and implementing the PySEBAL model (Figure 5). All of the spatial and temporal processing were performed in GRASS GIS 7.8 software which is an open-source and available under GNU General Public License (GPL).

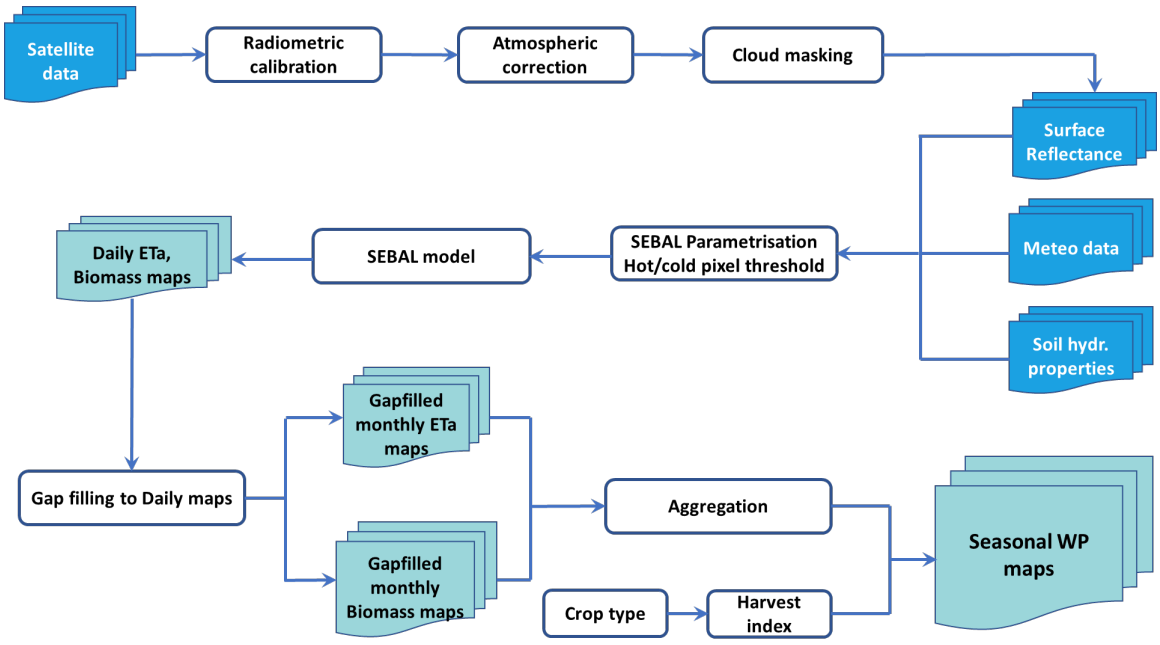

Figure 5: The PySEBAL methodological framework for WP assessment

21. PySEBAL is a python library to implement SEBAL from spatial data including spectral reflectance, climatic parameters, and altitude as inputs to estimate the surface energy balance components (Bastiaanssen et al., 1998a, 1998b). The outputs include parameters related to vegetation, energy balance, biomass, ET, and water productivity (Jaafar and Ahmad, 2020).

22. PySEBAL is provided as an open-source library with Apache version 2 license in a GitHub repository (https://github.com/wateraccounting/SEBAL). Currently, PySEBAL supports input data from the MODIS, Landsat, and Proba-V satellite sensors which facilitate the production of daily and seasonal ET_a maps. For this case study, PySEBAL was used to compute ET_a and AGBP maps over the KPIS for the Landsat acquisition dates from September 2016 to June 2019. The theory behind PySEBAL to compute ET_a and AGBP is explained in detail in the project methodology document manual (Mul et al., 2020).

1. Gap filling of ET_a and AGBP maps

23. Landsat 8 has 16-days of re-visit time over a location. In an ideal situation there would be two observations per month per pixel; often this is not the case due to cloud cover. The first step in the gap filling procedure is to fill all of the gaps in the ET_a and AGBP maps which are due to lack of data as a result of cloud through an interpolation process. The process involves averaging the data over monthly intervals, and subsequently converting the monthly ET_a maps from mm/day to mm/month by multiplying each map by the number of days in the corresponding month. The averaged AGBP maps per month are also multiplied by the number of days in the corresponding month to estimate total monthly biomass production in kg/ha. The remaining gaps are finally filled using temporal and spatial interpolation.

24. The Locally Weighted Regression (LWR) based temporal interpolation method was employed to fill the gaps in monthly ET_a and AGBP maps using GRASS GIS 7.8 software (Metz et al., 2017). This method fits a time series model for each pixel in monthly raster images and interpolates the missing values using neighboring observations. Some gaps continue to persist in monthly maps after the application of the LWR temporal interpolation method due to insufficient valid observations in the time series. A bicubic spline based spatial interpolation which uses neighboring 16 pixels around the null pixel was applied to the individual LWR interpolated maps to fill the remaining gaps (Neteler, 2010). Gap filled monthly maps of ET_a and AGBP were aggregated (December to April) to derive seasonal outputs.

2. Yield and Crop water productivity calculations

25. Following the seasonal mapping of ET_a and AGBP, paddy yield was computed using the following equation:

$$Yield = \frac{AGBP * HI}{1 - MOI} \qquad \textit{Equation 1}$$

Where Yield is in kg/ha, AGBP is Above Ground Biomass Production in kg/ha, HI is Harvest Index and MOI is moisture content of the crop. Since paddy is the dominant crop in KPIS, HI value of 0.47 and MOI value of 0.12 were used in this study to estimate crop yield.

26. Following the calculation of crop yields, the crop water productivity is computed using the equation.

$$WP_c = \frac{Yield}{ET_a} \qquad \text{Equation 2}$$

Where WP_c is expressed in kg/m^3, yield in kg/ha, and ET_a is actual evapotranspiration converted into the volume of water per unit area in m^3/ha. To estimate biomass water productivity (WP_b), yield in the above equation will be replaced by AGBP.

27. The Relative Water deficit (RWD) index was used to identify areas that suffer the most from lack of irrigation water availability and access (Steduto et al., 2012). RWD is defined as

$$\mathrm{RWD} = 1 - \frac{ET_a}{ET_x} \qquad \text{Equation 3}$$

Where ET_x is the maximum crop evapotranspiration that has been calculated in this study by taking 99-percentile of specific crop ET_a

D. Results: Kamping Puoy

1. Crop water consumption (ET_a)

28. Monthly ET_a maps were aggregated from December to April to derive seasonal ET_a for KPIS for three irrigation seasons (2016/2017, 2017/2018, and 2018/2019; Figure 6). The data Figure 8 are presented at three different spatial scales; the first row shows the Et_a at the pixel level (30 m resolution); the second row summarizes the pixel level results for every 1 km canal length; and the third row summarizes the pixel level ET_a at the block level.

29. For all three years a west-east declining trend is apparent in the ET_a, indicating differences in water consumption between the head and tail reaches. This west-east declining trend is clearly visible in the aggregated ET_a maps at 1 km canal length. The command area served directly by the main canal and head reaches of secondary canals (SC 1-3) appears to have high ET_a values represented by a darker shade of blue. The agricultural land located up to 15km along the canal from the outlet have ET_a estimates in the range of 700 mm to 800 mm signifying adequate water supply to these locations. These areas may represent fields under cultivation in the irrigation season within the KPIS.

30. Areas with consistently low ET_a values are evident in the maps, represented by shades of yellow and brown; these are mostly located in the tail end of the secondary canals located close to Battambang Town. In 2016/2017, large sections of the irrigation blocks served by SC-2 and SC-3 located in the south and southeast demonstrate low ET_a values indicating low water availability in the reservoir during that period. Such consistent low ET_a in all three years may indicate fallow land due to inadequate water supply or the presence crops other than rice which have lower rates of water consumption.

31. Block level summaries and total water consumption for all three irrigation seasons are given in Table 6. The blocks which are served directly by the main canal (blocks A and B) show high ET_a estimates in the range of 700 to 800 mm. These two blocks, along with blocks F and H, located in the head reaches of respective canals, showed high seasonal ETa consistently across three mapped irrigation seasons. While the ET_a values for other blocks varied considerably between the seasons, possibly reflecting variable water supply, block G showed the lowest ET_a values with less variation across the three years. This is reflected in the low standard deviation values for block G (47.1 mm; *Table 3*). Even during the 2018/2019 season when the overall ET_a estimates were high for most of the command area, low ET_a persists in the tail end sections covered by blocks D and G. Such low water consumption even during this season of seemingly adequate water availability (2018/2019), indicates potential issues in the water distribution system to blocks D and G.

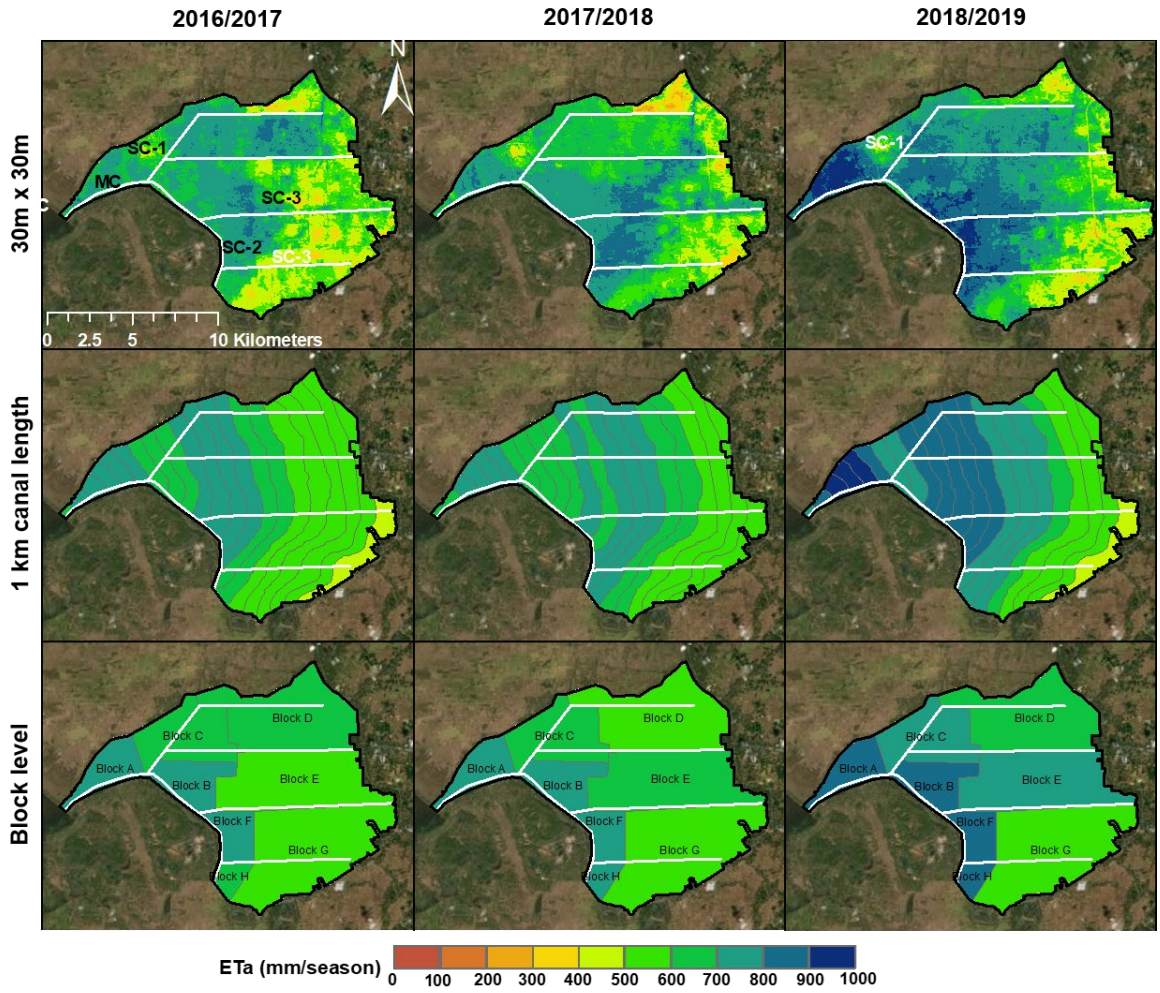

Figure 6: Seasonal ET_a maps of 2016/2017, 2017/2018, and 2018/2019 in the KPIS at different spatial scales.

Table 3: Block wise seasonal average ET_a and total water consumption

Blocks	Area (ha)	Seasonal average ETa (in mm)				Seasonal consumption (MCM)			
		2016/2017	2017/2018	2018/2019	SD	2016/2017	2017/2018	2018/2019	SD
Block A	762	710.0	731.5	886.9	96.5	5.4	5.6	6.8	0.6
Block B	918	701.5	720.6	828.4	68.4	6.4	6.6	7.6	0.5
Block C	1437	699.7	644.4	752.0	53.8	10.1	9.3	10.8	0.6
Block D	2446	661.4	576.2	672.7	52.8	16.2	14.1	16.5	1.1
Block E	2367	596.7	699.8	713.8	63.9	14.1	16.6	16.9	1.2
Block F	639	742.4	792.6	875.8	67.4	4.7	5.1	5.6	0.4
Block G	3150	515.9	598.3	596.5	47.1	16.3	18.8	18.8	1.2
Block H	281	673.9	776.9	831.3	79.9	1.9	2.2	2.3	0.2
Scheme	12000	625.0	650.0	709.0	43.1	75.0	78.0	85.1	4.2

32. The estimates indicate that scheme wide water consumption varied from 75 to around 85 MCM[1]. Blocks D, E, and G have higher water consumption (14 to 19 MCM) owing to their large size (*Table 3*). Block G is the biggest irrigation block in KPIS with an estimated command area of 3150 ha, located in the tail end of SC-3. The seasonal water consumption of block G is almost equal to that of the combined water consumption of blocks A, B, F, and H. Due to the smaller size of blocks A, B, F, and H, and their location near the head reaches of main or secondary canals, it is easier to satisfy it crop water requirement from the available.

2. Water Deficit Assessment

33. The RWD is used here as an indicator to identify and compare areas within an irrigation scheme that are affected by water availability. As a derivative of the crop water use within a command area, this index broadly indicates where irrigation water has been insufficient to meet the crop water requirement.

34. The RWD is presented in Figure 7 at three different spatial scales; the first row shows the results at the pixel level (30m resolution); the second row summarizes the pixel level results for every 1 km canal length; and the third row summarizes the pixel level ET_a at the block level. The spatial patterns in RWD demonstrate that areas closer to the main canal and head reaches of the secondary canals have a low water deficit (RWD = 0 to 0.3 represented by darker blue areas) in all three irrigation years. The tail end sections of the command area located in the south and southeast served by secondary canals SC-2 and SC-3 showed moderate water deficit (RWD = 0.3 to 0.6) in all irrigation seasons. The high RWD (>0.6) in the tail end sections were observed only in few patches across all three irrigation years. The scheme wide water deficit was lowest in 2018/2019 irrigation season. The large contrast between the moderate and low RWD between the head and tail end sections of SC-2 and SC-3 suggests unequal water distribution among the irrigation blocks served by the secondary canals. The tail end section of SC-1 shows a low water deficit in 2016/2017 and 2017/2018, and moderate deficit in 2017/2018. Most of the blocks experience moderate to low water deficit. In 2016/2017, only blocks E and G were above 30% water deficit while in 2017/2018 three blocks (C, D and G) were above 30% deficit. The results suggest that the water requirement of the blocks in the head reaches was mostly satisfied. Block G is the only block with consistently high RWD values in all three irrigation seasons.

[1] The ETa values should be used for relative comparisons; the absolute values should be treated with caution.

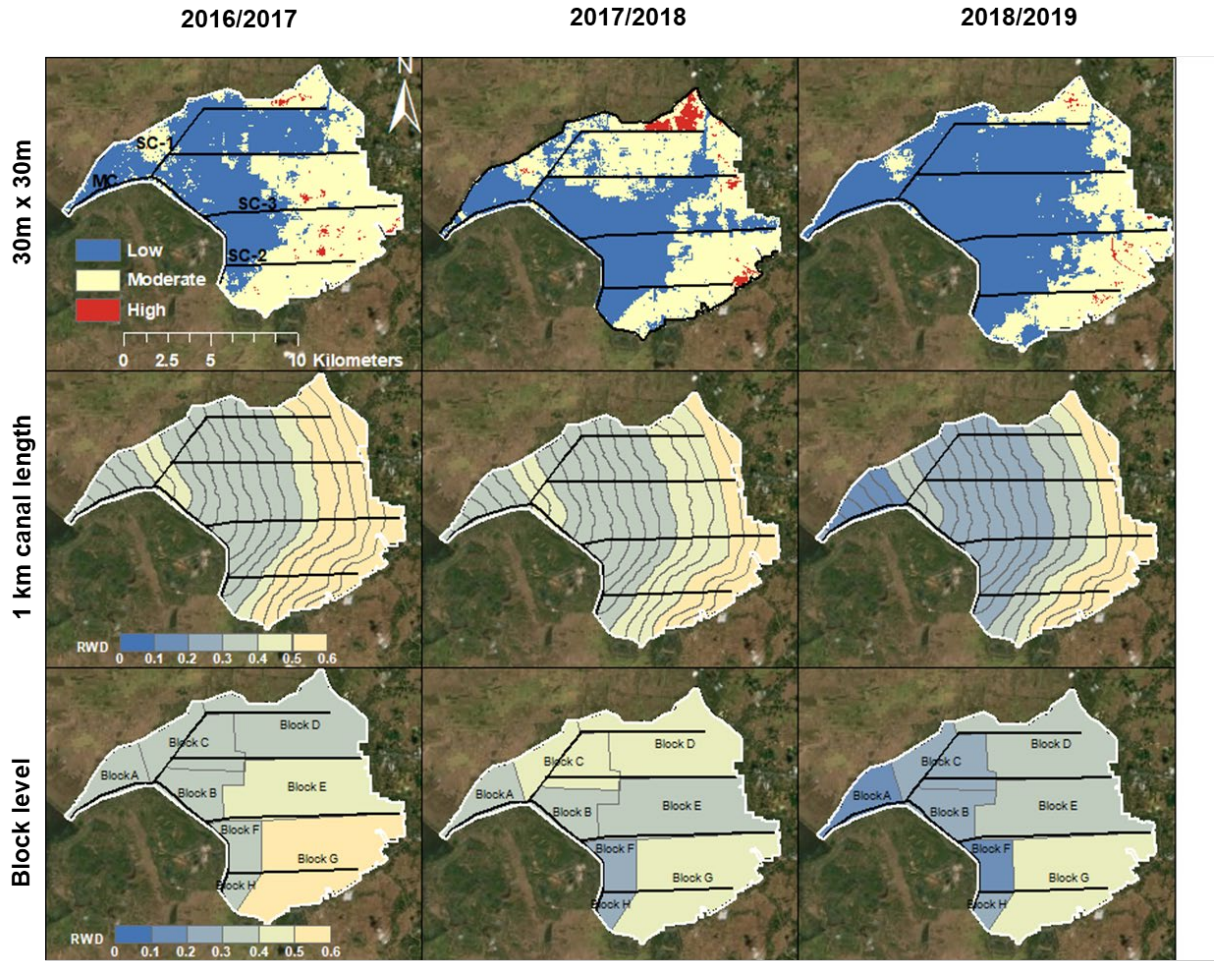

Figure 7: Seasonal RWD in 2016/2017, 2017/2018, and 2018/2019 in KPIS

3. Biomass production

35. The mean AGBP for each irrigation season was around 7,000 kg/ha for 2016/2017, 7,300 kg/ha for 2017/2018, and 7,560 kg/ha for 2018/2019. The spatial patterns are shown in Figure 10, for three different spatial scales. Both the pixel level maps (first row, Figure 8) and the 1 km canal length maps (second row, Figure 8) demonstrate large areas of with AGBP values below the seasonal mean. In 2018/2019, there is a clear head to tail difference in the AGBP estimates. While the seasonal average AGBP of 2018/2019 is closer to the other two seasons, the spatial pattern evident in both the 30 m pixel map and the 1 km canal length map clearly show crop growth in the 7 to 14 km reaches and intermittent cultivation mixed with fallow land (the red areas with very low AGBP values) in the tail end section.

36. The areas with high AGBP (green areas in Figure 8) are located mostly along the main canal or at the head reach of the secondary canals (SC-1, 2, and 3). The areas with the lowest AGBP (red areas in Figure 8) are mostly located in the tail end section of the secondary canals. In particular, the SC-2 tail end located in the south consistently shows large areas of low AGBP compared to the other two secondary canals (SC-1 and SC-3).

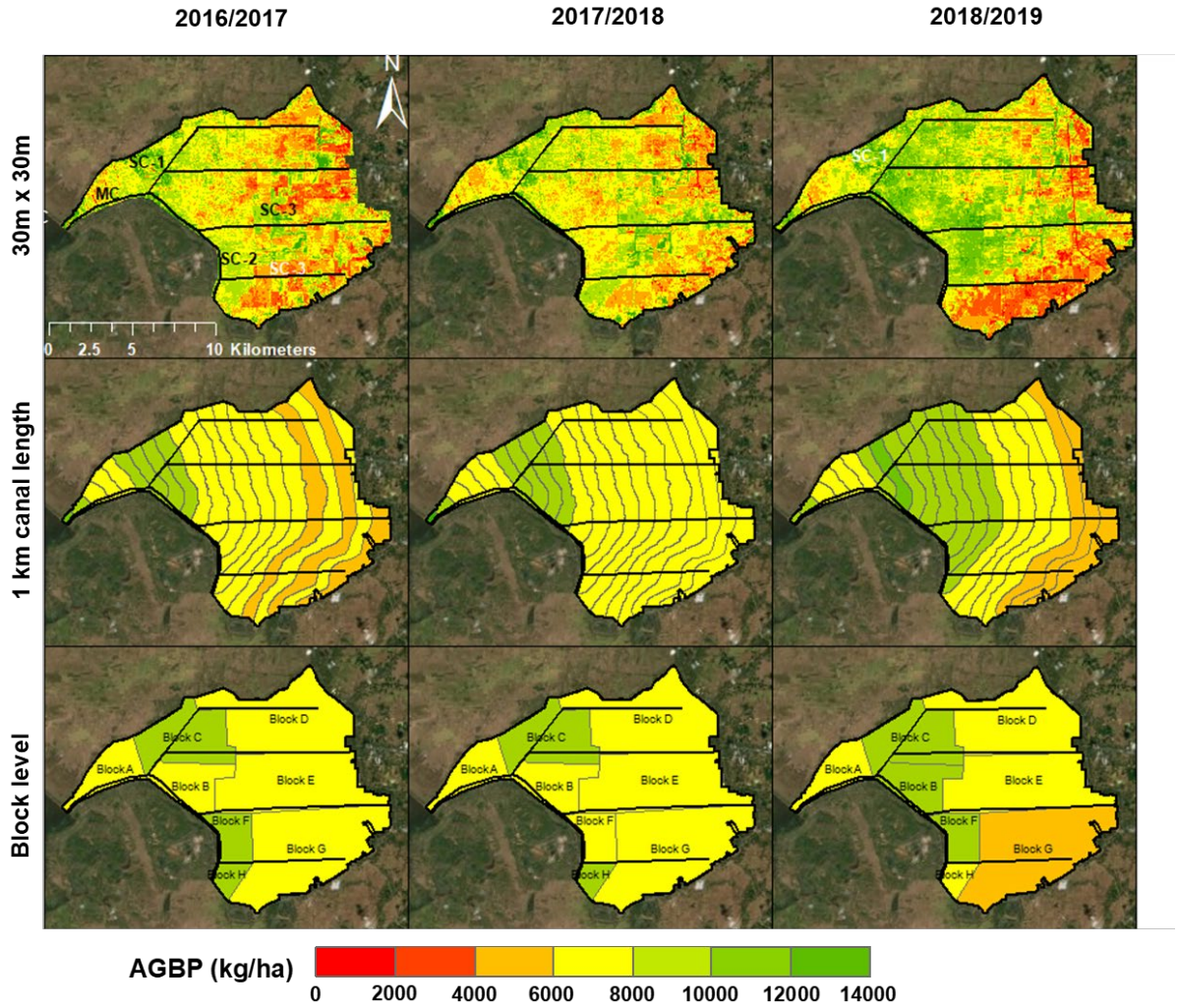

Figure 8: Seasonal AGBP maps of 2017, 2018 and 2019 irrigation season in the KPIS

37. The block level aggregation indicates two distinct clusters; i) blocks with average AGBP in the range of 8 to 10 ton/ha, and ii) blocks with AGBP in the range of 6 to 8 ton/ha. Block C was the only block which demonstrated consistently greater AGBP values for all three irrigation seasons. Blocks F and H served by SC-2 also demonstrated similar high biomass estimates for two irrigation seasons. Blocks A, D and E consistently range between 6 to 8 ton/ha of biomass production.

38. The inter-block variations were highest in the most recent irrigation season studied (2018-2019) ranging from lowest values (5.6 ton/ha) in block G at the tail, to highest values (9.8 ton/ha) in block F on the main canal. The very low AGBP in most of the tail end blocks possibly indicates sparse cultivation along with large areas of fallow land. In addition, the consistently low values across all three irrigation seasons suggests that either there was inadequate water availability in the reservoir to cover the entire command area of KPIS, or that the existing irrigation infrastructure was inadequate to distribute available water from the Kamping Puoy reservoir to tail end blocks.

39. The frequency distribution of AGBP values is shown in Figure 9 for all three irrigation seasons. The histograms confirm that during the 2016/2017 and 2017/2018 irrigation seasons, a significant portion of the command area display AGBP values lower than the seasonal mean (around 7 tons/ha). The distribution of values for 2018/2019 shows that many pixels lie in higher range of 8 and 10 tons/ha which is above the seasonal mean.

40. The large differences in AGBP estimates between the head reach and tail end blocks indicates potential scope for improvement through investments to ensure equitable resource distribution within the command area.

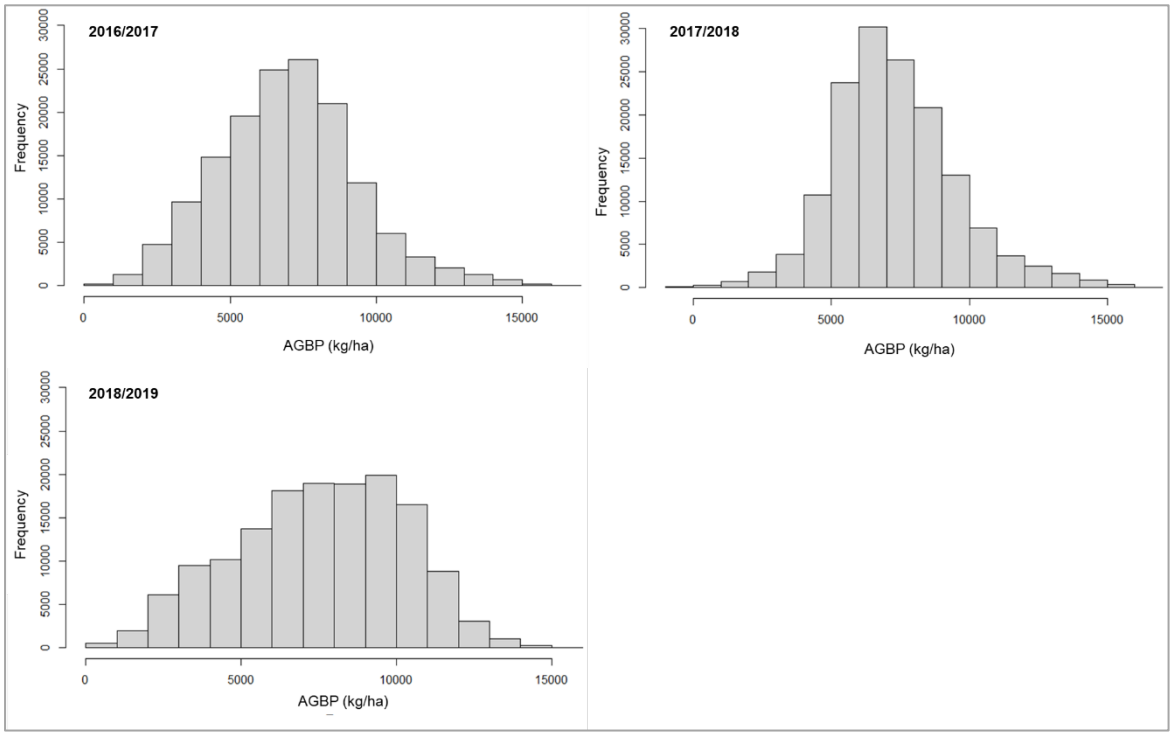

Figure 9: Histogram of the Biomass production (kg/ha) for KPIS for three irrigation seasons

4. Rice yield

41. Yield maps for paddy rice were developed by applying a crop specific Harvest Index (HI) to the AGBP outputs (Cai et al., 2009). These are presented in *Figure 10* and demonstrate that yields varied up to a maximum of 8.5 kg/ha.

42. At the scheme level, the highest average yield of 4 tons/ha was estimated for the 2018/2019 irrigations eason. The irrigation seasons of 2016/2017 and 2017/2018 demonstrated scheme average yields of 3.7 and 2.9 tons/ha. This is in line with values cited in the literature for ride paddy in Cambodia (IAIP, 2019; Mainuddin and Kirby, 2009). It should be noted that the seasonal average yield values also include locations of fallow land in the KPIS tail end which were not cultivated, since crop specific maps to separate cropped areas with fallow lands were not developed for this study. Most of the yield estimates fall within the range of 2-6 tons/ha which is consistent with the field reported observations of 3-5 tons/ha (IAIP, 2019).

43. Comparisons of the yield estimates in different sections of the command area indicate that the head reaches of SC-1 and SC-2, and the middle reach of SC-3 demonstrated yields greater than the scheme average. The head reaches of SC-2 and 3 showed larger intra-season variations in yield estimates of around 2 tons/ha between 2016/2017 and 2018/2019. The lowest average paddy yield was observed in the tail end section of secondary canals (SC 1-3).

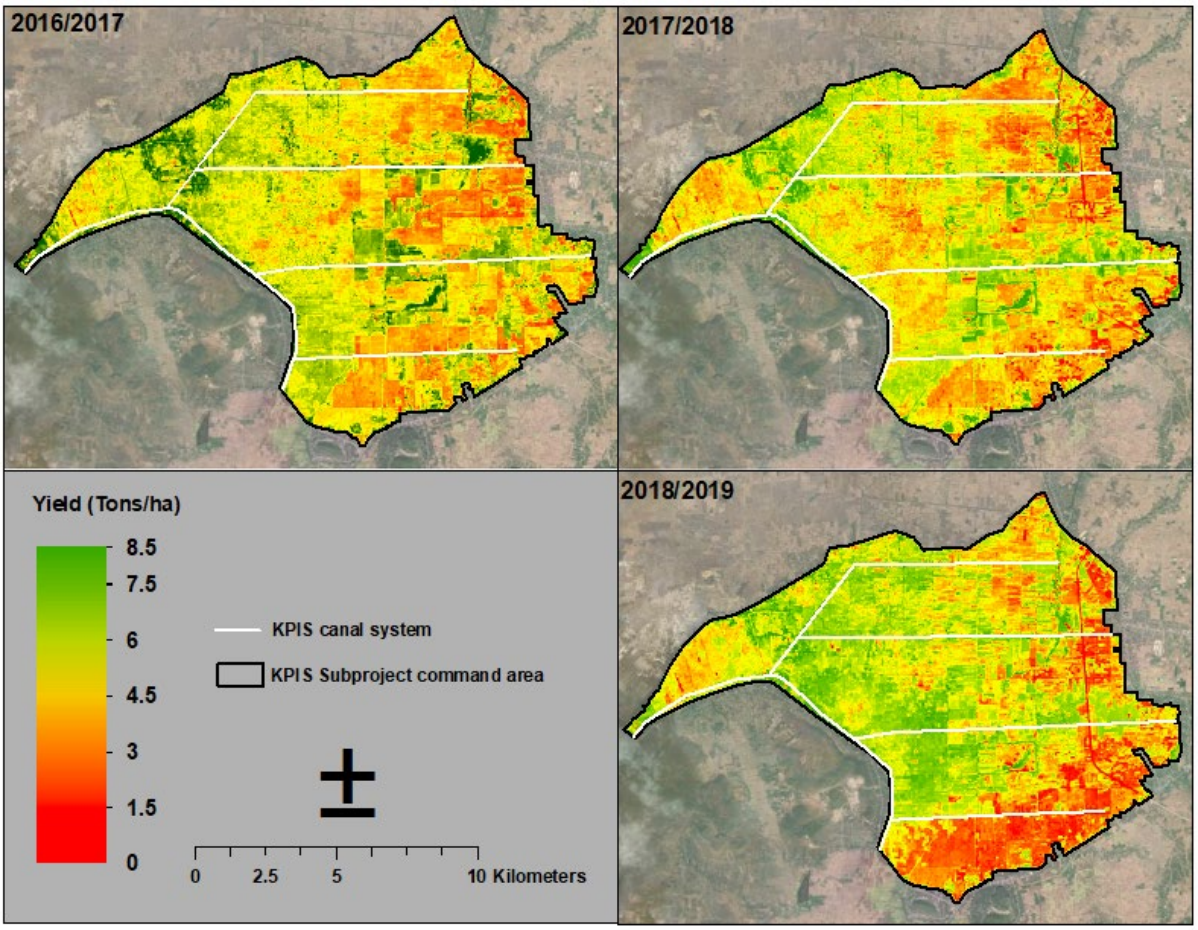

Figure 10: Yield map for paddy crop in the KPIS for three irrigation seasons

5. Rice specific water productivity

44. Crop Water Productivity (WP_c) was calculated for the KPIS as the crop specific yield per unit of ET_a (kg/m^3) (Blatchford et al., 2018). WP_c estimates for all three irrigation years show spatial variability within a narrow range of 0.1 to 1.2 kg/m^3 in the KPIS (Figure 11). The mean WP_c was 0.6 kg/m^3 with little variability between the three irrigation season.

45. The WP_c range in the areas where the AGBP values suggest that crops were planted during the seasons analysed, consisting of SC-1 to 3 head reaches and the area served directly by the main canal, is in the range of 0.4 to 0.8 kg/m^3. This is consistent with the reported crop water productivity range in Cambodia from other remote sensing based assessments (e.g. Mainuddin and Kirby, 2009).

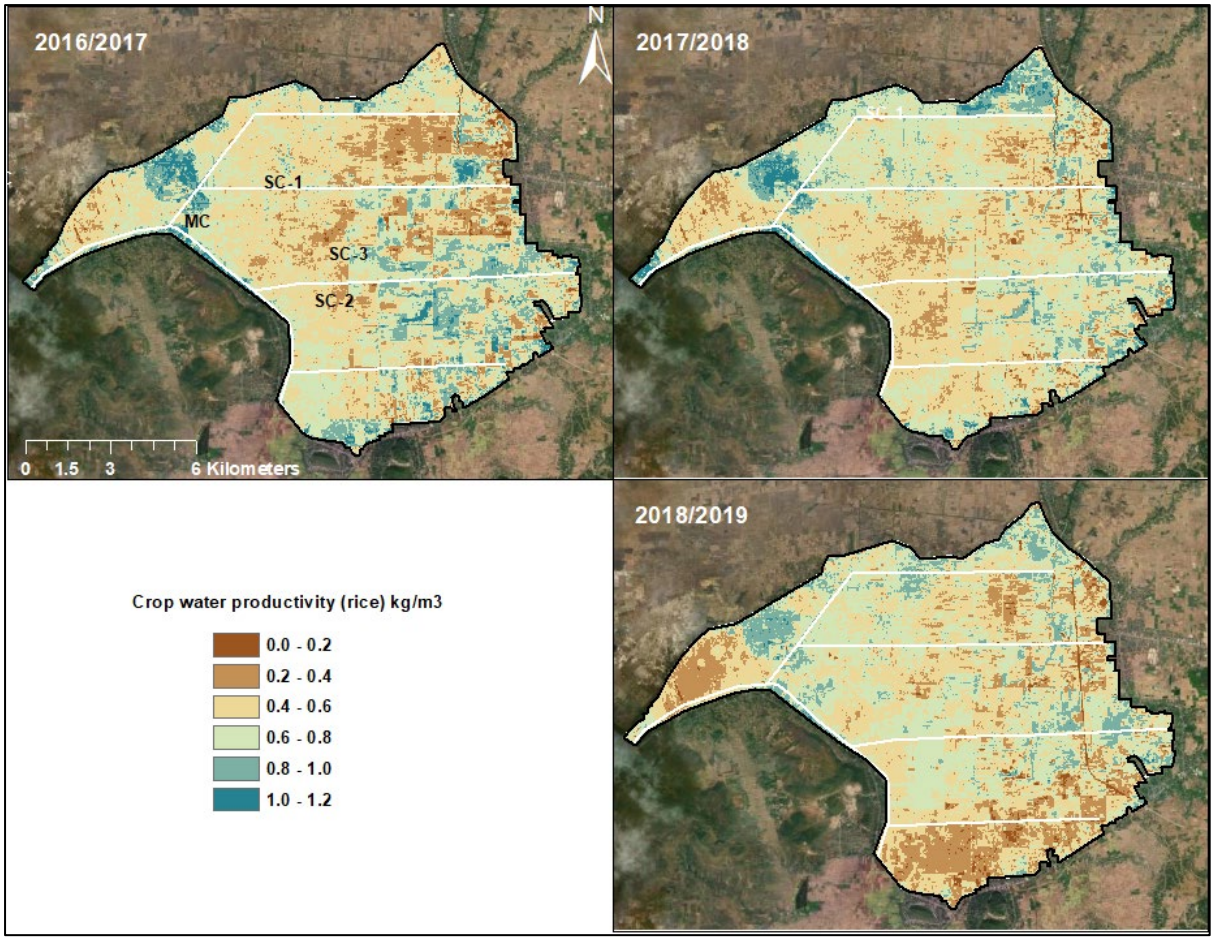

Figure 11: Crop water productivity for paddy in the KPIS over three irrigation seasons

46. As would be expected, the spatial distribution of WP_c does not follow the same patterns as the AGBP or ET_a. This is because the WP_c is a ratio of the AGBP over ET_a, hence, in calculations, areas with low AGBP and low ET_a will have a high WP and vice versa. Therefore, WP_c values should always be evaluated against these individual indicators and crop-specific yield information in order to find bright spots which represents optimal conditions in terms of production and water use (Cai et al., 2009).

47. The histogram of rice WP_c for the 2018/209 irrigation shows a unimodal distribution where the mean is around 0.57 kg/m^3 as shown in Figure 12. Based on the 95-percentile computed from the rice WP_c distribution, the possible potential target WP_c over the entire KPIS command area was found to be 0.86 kg/m^3. However, with targeted field based interventions irrigation water application this potential WP_c could be further improved.

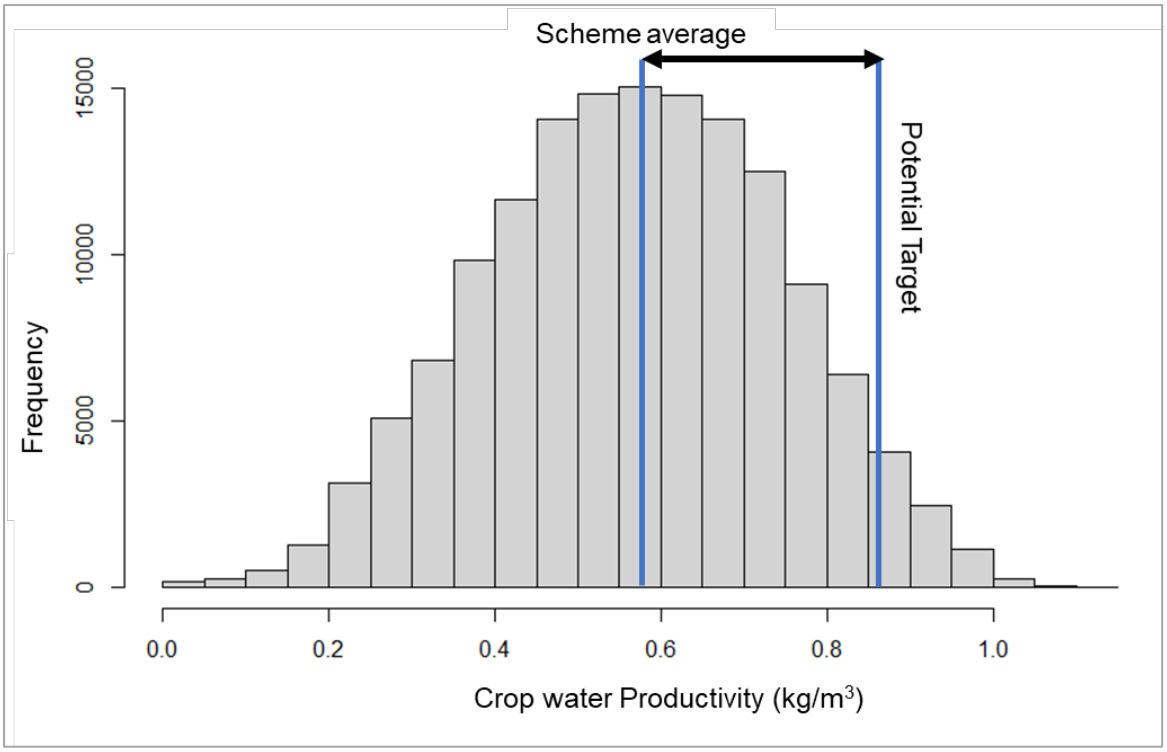

Figure 12: Histogram showing distribution of WP_c of rice in kg/m^3 over entire KPIS for the 2018/2019 season

E. Results: Stung Chinit Irrigation Scheme

1. Crop water consumption (ET_a)

48. Monthly ET_a maps were aggregated from December to April to derive seasonal ET_a for the SCIS spanning three irrigation seasons 2016/2017, 2017/2018, and 2018/2019. The seasonal mean ET_a for the SCIS varies from 445 to 566 mm, with the lowest being observed in 2018/2019 season. The variations in SD across the three irrigation seasons range from 101 to 106 mm. The SCIS consistently showed maximum ET_a values above 900 mm.

49. Distinct spatio-temporal patterns are evident in the seasonal ET_a values estimated for SCIS (Figure 13 – first row). The SCIS main canal has a north-south orientation deriving water from Stung Chinit reservoir in the North. High ET_a values (>600 mm) were consistently observed in the middle reaches of the SCIS in all three irrigation seasons closer to the western boundary. The spatial location of the low ET_a values varied over the years, with the head reach showing low ET_a in 2016/2017, the tail end in 2017/2018, and system wide low values in 2018/2019. The middle reach showed consistently high ET_a estimates in all irrigation seasons. These patterns suggest uneven availability or distribution of water within the irrigation scheme. As the irrigation scheme is not currently fully operational, the farmers in the middle reach either have better water distribution infrastructure from the main canal compared to head and tail end blocks or likely have access to other sources of water to meet irrigation needs. The current consumptive water use based on aggregated ET_a at the scheme level for each season was 142, 140, and 112 MCM respectively for 2016/2017, 2017/2018, and 2018/2019 irrigation season.

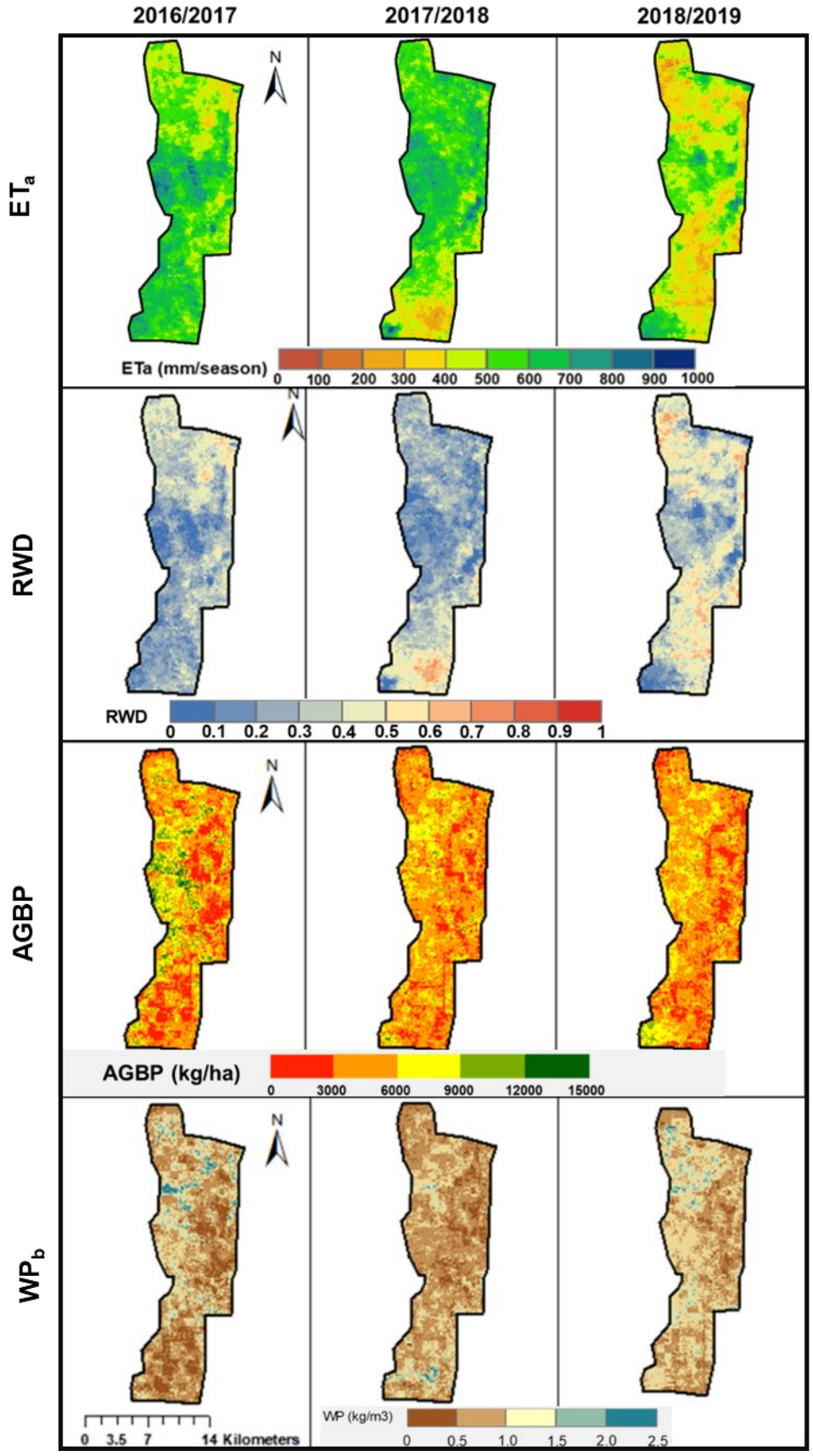

Figure 13. Seasonal ET_a, RWD, AGBP and WP_b in SCIS for three irrigation seasons

2. Relative Water Deficit

50. The RWD is used here as an indicator to identify and compare areas within an irrigation scheme that are affected by varying water availability and consistency in the water supply. As a derivative of the crop water use within a command area, this index broadly indicates where irrigation water has been insufficient to meet the crop water requirement. The mean, scheme wide RWD for SCIS was relatively low in all years, ranging from 0.29 in the first two irrigation seasons to 0.4 in the third season.

51. The spatial patterns of RWD estimates reflect the ET_a patterns (Figure 13, row 2). In SCIS, high RWD (> 0.7) locations were present in the head reach in 2016/2017, in the tail end in 2017/2018 and in both the head and tail end section in 2018/2019. Except a small cluster of high and moderate (0.3 to 0.7) RWD in the first two years, most of the SCIS scheme showed to low RWD (0 to 0.3). In contrast, in 2018/2019 most of the head and tail end sections located in north and south respectively showed moderate to high RWD. The middle section of the SCIS command area consistently showed low RWD.

3. Above Ground Biomass production

52. The ABGP patterns which can be seen in the SCIS command areas reflect those shown in the ET_a maps (Figure 13, row 3). In the SCIS, the areas which demonstrate high AGBP indicated by shades of green (<9000 kg/ha) were visible only in 2016/2017 irrigation season and were concentrated in the middle reaches in the western section of the command area. In 2017/2018 and 2018/2019 irrigation season, most of the command area showed AGBP less than 6000 kg/ha. Visual interpretation of high-resolution imagery indicates location of the main canal running north-south close to the eastern boundary of the SCIS command area. The locations of low AGBP happen to lie in the agricultural land located adjacent to the main canal. The patches of high AGBP seen in 2016/2017 in cropland may be a result of farmers tapping into other water sources such as local ponds and shallow groundwater to meet their irrigation requirements.

4. Biomass Water Productivity

53. Across the three irrigation seasons, the mean WP_b of SCIS varied between 0.8 to 1.2 kg/m^3. The spatial patterns of the WP_b in SCIS showed predominantly low water productivity (<1 kg/ m^3) during the first two seasons followed by moderate water productivity (1 to 2 kg/ m^3) in the third irrigation season (*Figure 13*, row 4). Only small patches of high water productivity (>2 kg/m^3) can be seen in all three seasons. In SCIS, estimates of high WP_b (> 2 kg/m^3) can be seen only in a few pixels during the 2016/2017 season. These pixels are located closer to the northwestern boundary of the command area. Most of the command area in the eastern section of the middle reaches and in the tail end showed WP_b values between 1 to 2 kg/m^3, while rest of the western middle reaches showed low WP_b. In 2017/2018 irrigation season, the head reach in the north and tail end in the south showed predominantly low WP_b values while middle reaches showed 1 to 2 kg/ m^3. Over the 2018/2019 season, the western half of the command area showed moderate WP_b values while the eastern half predominantly showed low estimates. In SCIS, the low WP_b values

observed in the first two irrigation seasons were a result of high ET_a and low AGBP estimates. Relatively lower ET_a values in 2018/2019 season along with low AGBP increased the overall water productivity in the SCIS.

F. Results: Prek Po Irrigation Scheme

1. Crop water consumption (ETa)

54. The seasonal mean ET_a varies from 358 to 456 mm for PPIS. The mean ET_a shows a decreasing trend over the three irrigation seasons with lowest values recorded in 2018/2019 (358 mm). This lowest value is substantially lower (~100 mm) than the mean ET_a of previous two years. The PPIS show greater variability between years, with the SD varying between 91 and 144. In PPIS, a was recorded for the 2018/2019 season.

55. The PPIS is currently not operational which is reflected in the system-wide low ET_a values (Figure 14 – row 1). The seasonal mean ET_a values range from 358 to 456 mm across the three seasons which is substantially lower than the seasonal mean ET_a values estimated for the other two schemes. Visual interpretation of a few isolated high ET_a clusters visible in the north using high resolution Google Earth reveals the presence of permanent vegetation. But the other high ET_a cluster located in the southeast of the scheme primarily consists of cropland. This may indicate that farmers in this area have access to additional water sources from the Tonle Touch river. The current consumptive water use based on aggregated ET_a at the scheme level was 42, 39, and 33 MCM respectively for 2016/2017, 2017/2018, and 2018/2019 irrigation season.

2. Relative Water Deficit

56. For PPIS, the mean RWD for the three irrigation seasons was 0.37, 0.45, and 0.48. In PPIS, no apparent high RWD areas were noticeable in 2016/2017 and a small high RWD cluster in the east in 2017/2018 (Figure 14 – row 2). In 2018/2019, three distinct high RWD clusters were seen in east, west and south. In addition, the areas adjacent to the main canal which runs in a north-south direction consistently showed high RWD across the three irrigation seasons.

3. Above Ground Biomass production

57. The mean AGBP across the three irrigation seasons varied between 4,700 and 5,234 kg/ha in SCIS, 3,600 to 5,244 kg/ha in PPIS. In PPIS Figure 14 – row 3), low AGBP (< 3000 kg/ha) dominates the 2016/2017 irrigation season. The spatial patterns in 2017/2018 showed patches moderate AGBP (6000 to 9000 kg/ha) in the north close to the Mekong River and in the center of command area. These locations with moderate AGBP are visible as yellow patches amid low production areas (indicated in red). These locations may indicate isolated areas of cultivation within the PPIS command area. Apart from a small section of lands located close to the command area center, most of the PPIS showed low AGBP values in 2018/2019 irrigation season. These results are consistent with the findings from the IAIP (2019b), which describe the crippling state of irrigation infrastructure in PPIS.

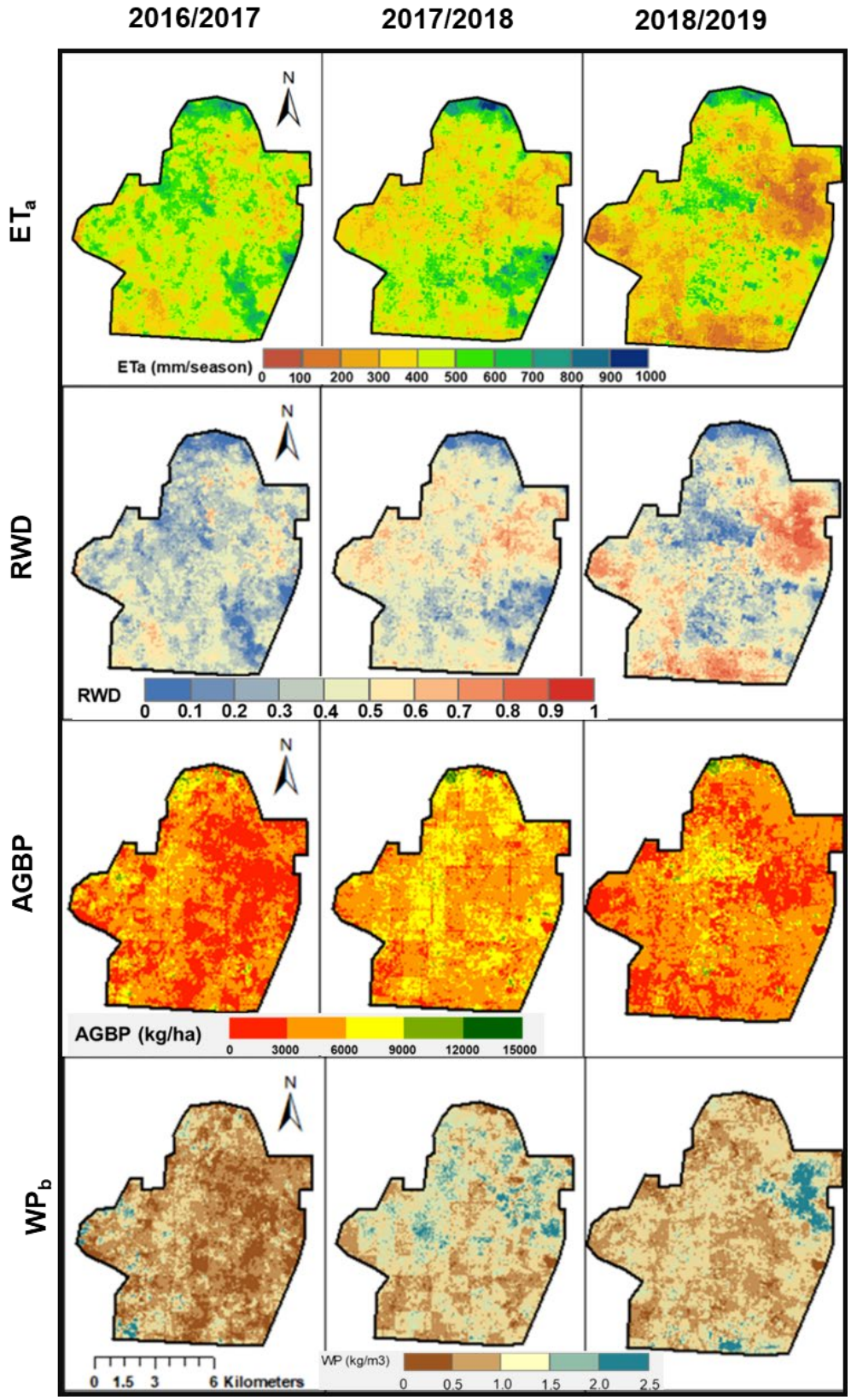

Figure 14: Seasonal ET_a, RWD, AGBP and WP_b in PPIS for three irrigation seasons

4. Biomass Water Productivity

58. The mean WP_b of 0.8 to 1.2 kg/m^3 PPIS. The head and middle reach sections of PPIS showed different WP_b estimates in every season varying from low to high in the two seasons followed by moderate WP_b (Figure 14 – row 4). The tail end sections varied from low to moderate WP_b. High WP_b is noticeable in the second and third season in the sections closer to the eastern command area boundary. For PPIS, low WP_b dominate the eastern half of the command area while 1 to 2 kg^3 were estimated widely for pixels in the western side in the 2016/2017 irrigation season. Over the 2017/2018 season, a small cluster of high WP_b was noticeable close to the eastern command area boundary while head and middle reaches predominantly showed 1 to 2 kg/m^3 followed by low WP_b were seen in the tailend. followed by higher values across the scheme in the next two years. The WP_b spatial patterns in 2018/2019 consist of high WP_b values in the east, moderate values concentrated around the center and western boundary and, low WP_b in the rest. The first and third irrigation season under consideration showed large area of biomass production less than 3000 kg/ha having moderate ET_a resulted in low WP_b (>1 kg/m^3) dominating major part of the command area. These locations were likely fallow due to limiting factors from inadequate water supply. The second irrigation season saw increased biomass production for similar ET_a estimates leading to high WP_b. Some crop cultivation in the second irrigation season cannot be discounted.

G. Results: Canal 15 Irrigation Scheme

1. Crop water consumption (ET_a)

59. Monthly ET_a maps were aggregated from December to April to derive seasonal ET_a for the C15IS spanning three irrigation seasons 2016/2017, 2017/2018, and 2018/2019. The seasonal mean ET_a varies from 515 to 717 mm for C15IS. Overall, crop water consumption was consistently highest in the C15IS among the three irrigation schemes along the Mekong river. The daily average ET_a in rice fields in South and Southeast Asia is expected to range from 4 to 7 mm/day (Tomar and O'Toole, 1980); in Cambodia, the dry season rice growing period is around 130 days (Mainuddin and Kirby, 2009), which amounts to an estimated crop water requirement ranging from 520 to 910 mm/season. The estimated mean ET_a for all three irrigation schemes (the calculated range of 515 to 717 mm/season from the remote sensing data) falls within this range. Due to the flooded nature of some of these irrigation schemes, ET_a and resultant crop water productivity may vary.

60. C15IS show greater variability between years, with the SD varying between 108 and 144 mm respectively. The largest difference in seasonal mean ET_a between irrigation seasons (an overall increase of 202 mm from 515 to 717 mm) was observed in the C15IS irrigation scheme between the 2016/2017 and 2017/2018 irrigation seasons. The largest difference in seasonal mean ET_a between irrigation seasons (an overall increase of 202 mm from 515 to 717 mm) was observed in the C15IS between the 2016/2017 and 2017/2018 irrigation seasons.

61. The seasonal ET_a maps of the C15IS (Figure 15 – row 1), indicate large sections of the command area with high ET_a values (>600 mm). These are located in the section of the command which is served by C15IS and Canal 87. The highest seasonal ET_a values recorded within the scheme (>800 mm during 2017-2018) are also located in this area. The high ET_a values were due to the saturated conditions of the agricultural land during the initial period of irrigation seasons. This location is a part of Mekong floodplains and was observed to be under flood submergence during the monsoon season. In contrast, consistently low ET_a values are evident in the south of the scheme during all three irrigation seasons; this is the upland area served by the Sampot pumping station. The total water consumed in the C15IS ranged from 50, 70, and 59 MCM respectively for 2016/2017, 2017/2018, and 2018/2019 irrigation seasons.

62. In contrast to the other two irrigation schemes along the Mekong river, in C15IS the lowest seasonal mean ET_a (515 mm) was observed in 2016/2017, and not during the 2018/2019 irrigation season. The main canal of C15IS is directly connected to the river system, the water availability within the irrigation scheme is heavily influenced by the dynamic changes in river water levels. Low water levels in the river in the 2016/2017 irrigation season might thus have contributed to low water availability in the C15IS. The estimated declining temporal trend apparent in SCIS and PPIS ET_a patterns are consistent with the declining monsoon rainfall trend from 2016/2017 to 2018/2019 season. However, such similar ET_a-rainfall trend is not noticeable in the C15IS.

2. Relative Water Deficit

63. For C15IS, the mean RWD for the three irrigation seasons were 0.2, 0.18, and 0.28 respectively. In the C15IS irrigation scheme, most of the lowland command area served by C15IS and its secondary canal Canal 87 have low water deficits (blue areas, Figure 15 – row 2). There is an area with consistently high deficits noticable in all three irrigation seasons (the yellow and red areas, last row in Figure 16) located in the south. This upland area is served by Sampot pumping station. Over 70% of the pixels which exhibit a high deficit are located in the sub-command area served by the Sampot pumping station. This broadly indicates that irrigation water was insufficient to meet the crop water requirement in the uplands area within the C15IS. It should be noted that the RWD estimates particularly for the lowland areas will be heavily influenced by the duration of the flood pulse within the C15IS command area. In 2016/2017 and 2017/2018, large sections of the lowland command area appear to have large ET_a values possibly because of prolonged flooding from the previous monsoon season.

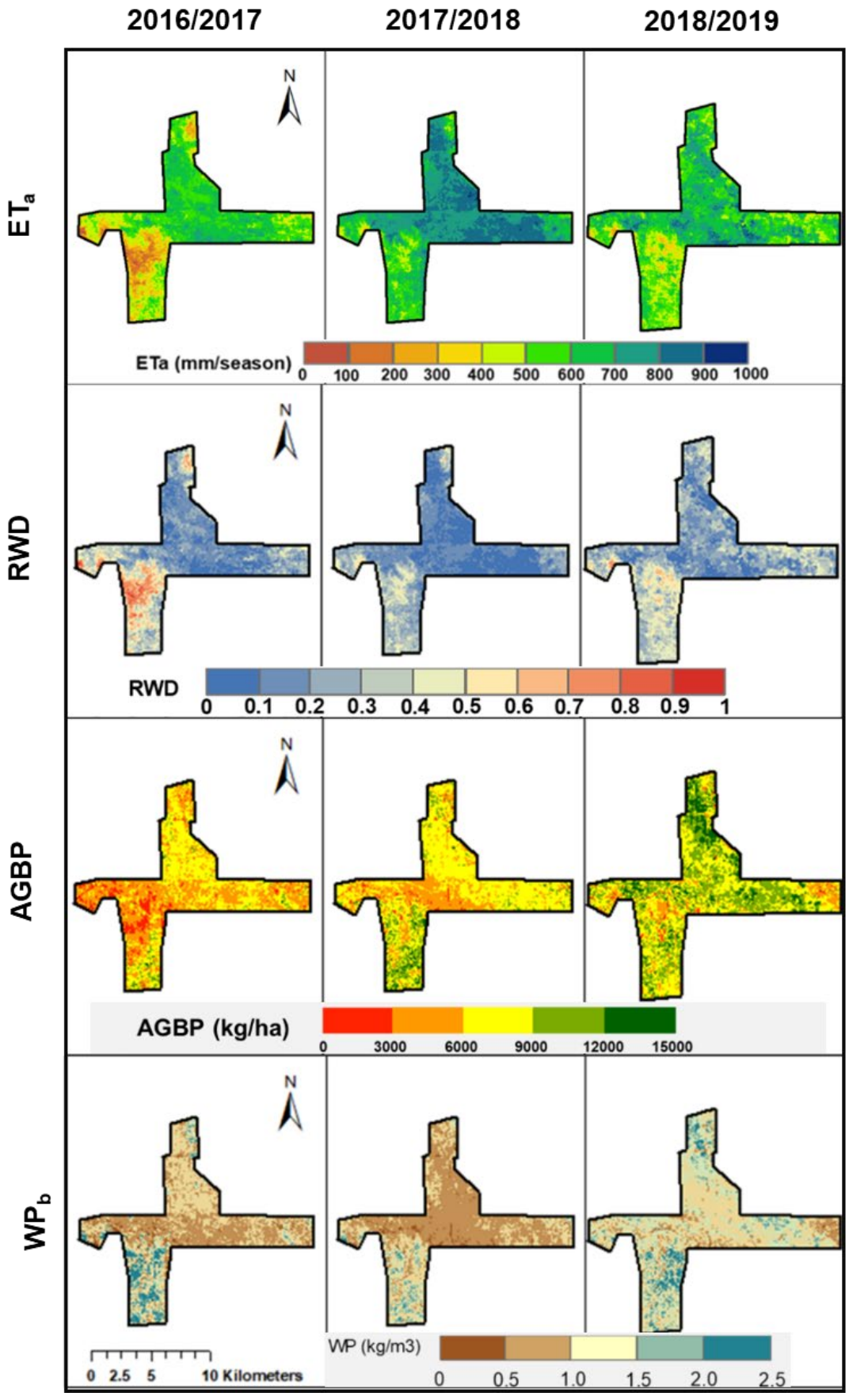

Figure 15: Seasonal ETa, RWD, AGBP and WPb in C15IS for three irrigation seasons

3. Above Ground Biomass production

64. C15IS showed consistent high AGBP values across three irrigation season (Figure 15 row 3). Most of the C15IS showed values in the range of 6,000-15,000 kg/ha (yellow to green areas). These values align with other AGBP estimates in the region, for example from the paddy dominated Kamping Pouy Irrigation scheme. In C15IS, farmers must wait for floods to recede to initiate agriculture activities in December. In 2017/2018, C15IS command areas were saturated even in late December and early January possibly due to a prolonged flood pulse. This would have led to the delayed onset of the irrigation season in 2017/2018. Saturated conditions within the command area during the initial phase of irrigation season would contribute to high ET_a estimates. The moderate AGBP estimates (6,000 to 9,000 kg/ha) could be due to reduced planting. The high spatio-temporal variability of AGBP seen in the 2018/2019 season suggests a significant potential to improve production rates within the C15IS command area through improved drainage to facilitate timely planting of crops after the monsoon season and investment in irrigation infrastructure to ensure delivery to the tail end.

4. Biomass Water Productivity

65. The WP_b in the lowland command area in the east-west direction varied from low for the two seasons, to a mixture of moderate to high in the third irrigation season (Figure 15 – row 4). The lowland command area in the north followed a pattern of predominantly moderate and low in the first two irrigation seasons to a mix of moderate to high WP_b in the third. The upland command area generally showed large clusters of higher WP_b in the first and third irrigation seasons. In C15IS, low values of WP_b (0 to 1 kg/m^3) were seen in lands adjacent to the main canal in east-west direction in the 2016/2017 irrigation season. The northern section of the command area which forms the middle reach showed moderate WP_b values, while the southern section representing the tail end showed a mix of high and moderate WP_b.

66. In 2017/2018 irrigation season, low values dominate the head and middle reaches, while moderate WP_b values were seen in tailend upland section forming the southern portion of the command area. Except for a few patches of land in the tailend showing high WP_b values, most of the command area showed moderate WP_b. During the first two irrigation seasons, high ET_a but low to moderate AGBP limited the WP_b in head and middle reach of the command area. An exception to this being the tailend which showed high WP_b due to lower ET_a but with low to moderate AGBP values. While the AGBP patterns remained similar, a clear positive change in the AGBP pattern was visible in 2018/2019 compared to the two previous years. With similar water consumption in the command area but higher AGBP in 2018/2019 resulted in scheme wide increase in overall water productivity. Low WP_b seen in C15IS command area across irrigation years could be attributed to the high ET_a values from the presence of standing water following flood recession at the start of the growing season. Increased biomass production but with similar ET_a estimates like previous year contributed higher WP_b.

5. Rice yield and crop water productivity

67. Yield maps (Figure 16) were developed by applying a crop specific Harvest Index (HI) to the AGBP estimates, following Equation 1. At the scheme level, the highest average yields

(4.6 tons/ha) were produced during the 2018/2019 season. Lower yields of 3 and 3.7 tons/ha were calculated for the 2016/2017 and 2017/2018 seasons respectively. The large variations in yield between different years is likely due to water availability in the river to which C15IS is directly connected, and which also influences flood patterns during the wet season which in turn determines the duration of irrigation season.

68. The maps (Figure 16) indicate that yields typically fall within the range of 2-6 tons/ha (the yellow and light green areas) which is consistent with field reported observations (3-5 tons/ha; IAIP, 2019c). Comparing the paddy yield estimates in different sections of the command area indicates a clear head-tail (east-west) difference in 2016/2017 and 2017/2018. This spatial pattern was not evident in 2018/2019 possibly due to adequate water availability to cover most of the lowland command area which spans in east-west direction between Angor Borei and Takeo towns. From the temporal patterns, it is apparent that the water availability from the river has bigger impact on crop production since 2018/2019 season showed adequate distribution of high ET_a, AGBP and yield estimates throughout the command area. There might still be distribution issues from delivering water from the main canal to the distant farmlands. Since the cropping season is heavily influenced by the duration of flood pulse in the Mekong river, it is imperative to provide enough drainage facilities within C15IS command area to facilitate irrigation activities.

69. The rice yields were generated only for C15IS irrigation scheme and not for SCIS and PPIS. The seasonal biomass production estimates for SCIS and PPIS were lower than the typical biomass production expected from the paddy crop. Since major sections of SCIS and PPIS command area likely remained fallow, any yield estimated would be meaningless.

70. Large inter-year variations in yield were observed in upland command area located southeast of Takeo town and served by the Sampot pumping station. Low yields (< 2 tons/ha) were observed in 2016/2017 followed by a progressive increase in yields over the next two irrigation seasons. The locations of high RWD (water deficits) seen in Figure 7 coincide with locations of low yield estimates in the C15IS upland command area. Further block level analysis may identify the inter and intra-canal yield variations in different sections of the command area.

71. Based on the yield data and the water consumed, the crop water productivity (WP_c) was calculated for the C15IS as paddy yield per unit of ET_a (kg/m^3; Figure 17). For the 2016/2017 and 2017/2018 irrigation seasons, high ET_a coupled with low to moderate yield led to low WP_c (the orange areas, Figure 20). Except for the uplands, located in the southern portion of the command area, most of C15IS has WP_c values in the range of 0.2 to 0.6 kg/m^3. The 2018/2019 irrigation season demonstrates a substantial increase in WP_c (0.6 to 1 kg/m^3) compared to the earlier two seasons.

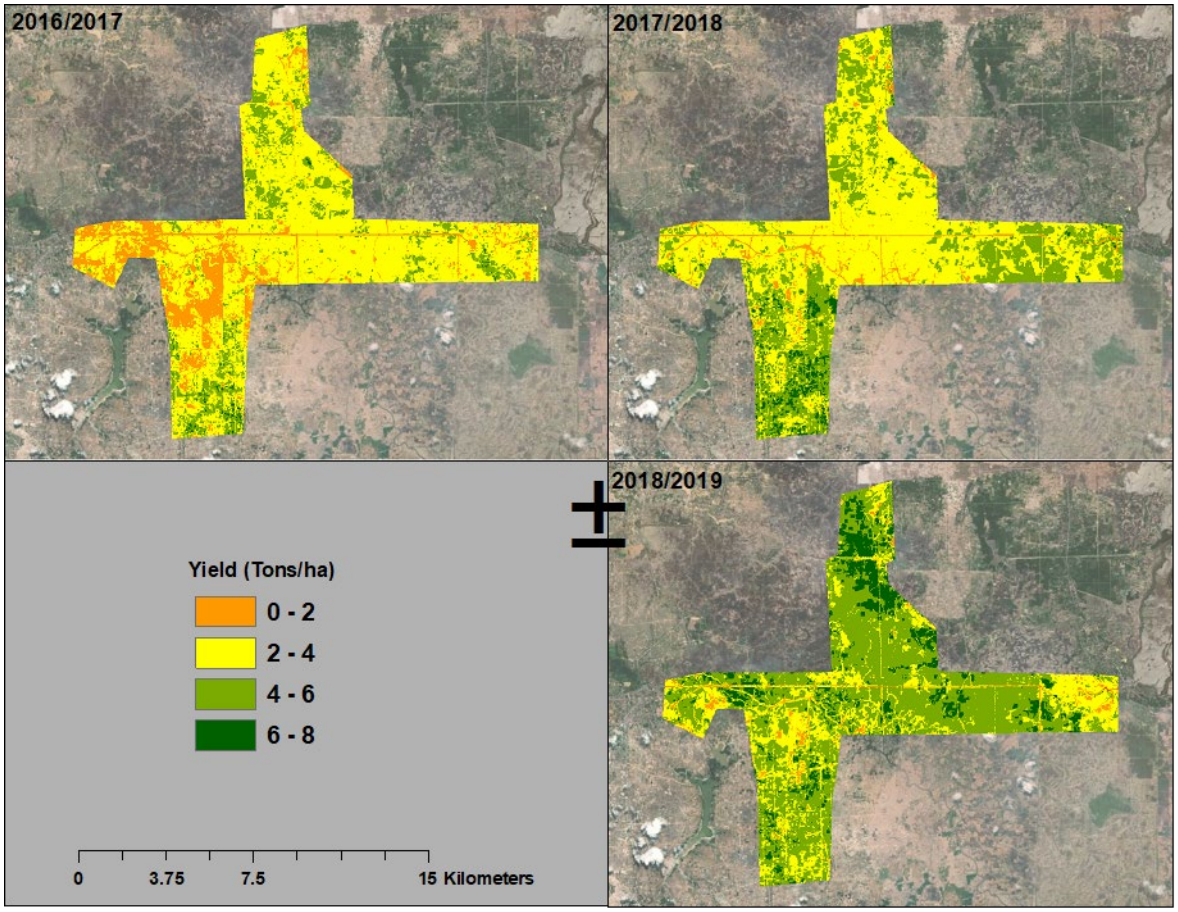

Figure 16: Rice yield map for the C15IS over three irrigation seasons between 2016-2019

72. The high WP_c observed in the upland command area served by the Sampot pumping station was primarily due to low ET_a values, possibly indicating unequal water distribution between the upland and lowland command area. The ET_a, AGBP, yield and WP_c estimates are heavily influenced by the flood recession agriculture practiced in the command area. A marginal change in the flood pulse pattern may impact crop cultivation activities by influencing the available timeframe for the irrigation season. Some of the low WP_c could be a result of high ET_a during the initial irrigation months when flood waters are still present. Provision of flood protection and drainage facilities will aid farmers to promptly start dry season cultivation November/December, which will also improve the overall water productivity of the C15IS irrigation scheme by reducing ET_a from stagnant water.

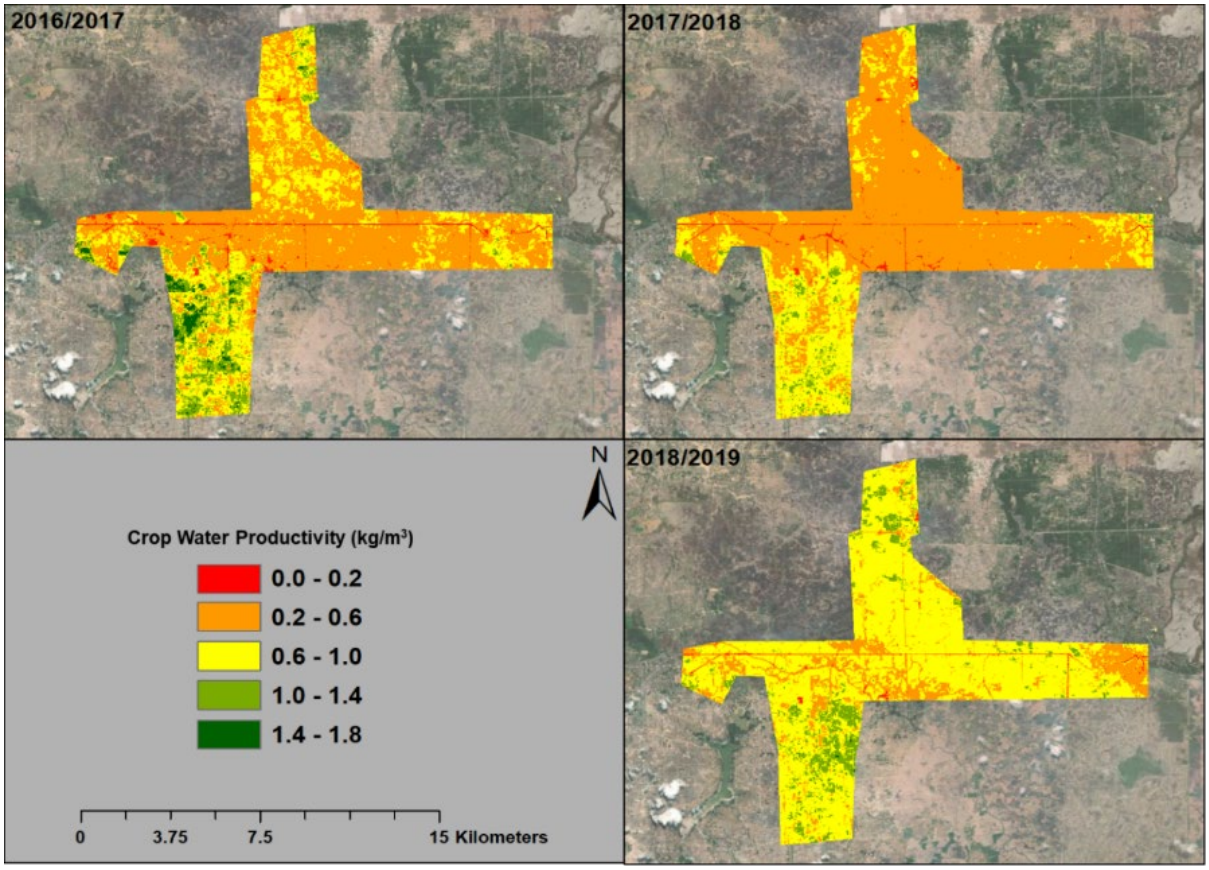

Figure 17: Crop water productivity (WP_c) calculated for paddy in the C15IS over three irrigations seasons, from 2016-2019.

IV. SUMMARY AND KEY FINDINGS

73. A water productivity study has been undertaken for four irrigations schemes in Cambodia; KPIS, SCIS, PPIS, and C15IS covering three irrigation seasons from 2016/2017 to 2018/2019. These schemes located in located in the Battambang, Kampong Cham, Kampong Thom, and Takeo provinces are the Subprojects of the Irrigated Agriculture Improvement Project (IAIP), proposed by the Ministry of Water Resources and Meteorology (MOWRAM) of the Royal Government of Cambodia (RGC), for loan funding by the Asian Development Bank (ADB). IAIP will assist the Government of Cambodia to modernize and improve the climate and disaster resilience of these irrigation systems; this will include rehabilitation of canals to ensure water delivery.

74. The KPIS irrigation blocks in head reaches showed high ET_a in the range of 700 to 800 mm, which is enough to satisfy the crop water requirement of paddy crop. Even the tail end blocks showed ET_a in the range of 500 to 600 mm. However, estimated seasonal biomass production was in the range of 6 to 9 ton/ha, which significantly lower when compared with the biomass production estimates from paddy dominant irrigation schemes.

75. Overall water deficit within the command area of KPIS was less than 10 to 40 %. The head reach blocks showed a low water deficit while the tail end blocks of D, E, and G varied in response to the water availability and supply. Block G was the only block that showed a consistent water deficit of around 40%.

76. The inference from low beneficial fraction and low biomass production estimates point to 22 to 30 % crop coverage and presence of large tracts of fallow land in the KPIS. during the three irrigation seasons under consideration. Low irrigation coverage despite adequate water availability suggest that issues exist in conveyance and supply of irrigation water to different blocks from the reservoir outlets. There exists unrealized potential within the command area to physically expand paddy cultivation through targeted investments in irrigation in infrastructure for equitable water supply.

77. The average seasonal yield of paddy over the entire KPIS scheme for the three irrigation years was found to be 3.7, 3.9, and 4 tons/ha respectively. Corresponding scheme wide seasonal average crop water productivity estimate was around 0.6 kg/m^3. However, yield estimates varied substantially between head reaches and tail end sections of different secondary canals, and between different irrigation years.

78. The estimated mean ET_a was within the range of 445 to 566 mm across the three seasons. Most of the SCIS command area showed low AGBP estimates (< 6,000 kg/ha). The lower AGBP values may indicate farmers cultivating crops other than paddy due to reduced water availability in different parts of command area. The small clusters with moderate to high AGBP values may indicate farmers using other sources of water for irrigating their crops. The moderate ET_a and corresponding low AGBP values result in low water productivity estimates (< 1 kg/m^3) for large parts of the command area. In SCIS, large sections of canals are dilapidated because of poor maintenance, which significantly undermines the carrying capacity of the canal network. As a result, during the dry season cultivation is concentrated in small pockets along or close to the main canal owing to lack of water availability Farms

along the main canal have preferential water access compared to farms experiencing water shortages located far from the main canal.

79. Large sections of the PPIS command area consistently showed low ET_a values (below 400 mm) in all three seasons and low AGBP (6,000 kg/ha) in the 2016/2017 and 2018/2019 seasons. Low ET_a and lower AGBP values resulted in scheme wide low water productivity estimates (< 1 kg/m^3). The PPIS also suffers from inadequate irrigation water supply to different parts of the command area. Except for the parcels of land evident in the 2017/2018 irrigation season, water productivity remained low throughout the scheme (<1 kg/m^3). In addition, large areas of the cultivable land in PPIS likely remained fallow during the three years studied. The PPIS has not been operational since 2015 due to reduced efficiency and high operating cost of the pumping system and poor conditions of the canal networks. Farmers in the PPIS undertake agricultural activities mainly during the rainfed season

80. The C15IS showed high temporal variability of mean ET_a which ranges from 515 to 717 mm. The AGBP estimates varied from 9,000 kg/ha in the first two irrigation seasons, to 12,000 kg/ha in the third season. The magnitude of AGBP increase in 2018/2019 suggest that the command area supports extensive paddy cultivation during this season. This would need to be confirmed through further field assessments. Paddy yields for the first two irrigation season was in the range of 2 to 4 tons/ha but increased upto 4-6 tons/ha in 2018/2019. The tail end section of C15IS demonstrated consistently higher water deficits compared to the head and middle reaches. This tail end section is an upland area served by a separate pumping station. For the first two irrigation seasons, the crop water productivity of most of the command area was in the range of 0.2 to 0.6 kg/m^3; this increased to 0.6 to 1 kg/m^3 in the third irrigation season.

81. In C15IS, increasing water productivity particularly in the fields along the main canal has the potential to increase water availability for the tail end command area including the upland Sampot pumping station. The water deficits locations observed in the upland command area were not uniform and varied between the three irrigation seasons. While variations exist in water availability between the uplands and lowlands within C15IS, the exact reason could not be readily established and requires further assessment. Issues might exist with existing pumping infrastructure at Sampot, reduced water availability in the main canal for pumping, or a combination of both. The derived outputs must be further validated with stakeholders to identify the state of agricultural activities in the irrigation season, other crop types in the command area, and the use of supplementary water sources for cultivation.

82. Since most of the C15IS command area are within the Mekong floodplains and traditionally practice flood recession agriculture, duration of flood pulse has a major impact on the period available for the growing season. Prolonged flooding in C15IS lowland command area postpones the beginning of agricultural activities and reduce the available growing season time frame. Provision of flood protection along with adequate drainage facilities in the C15IS command area will ensure availability of cultivable land in timely manner and reduce the uncertainties associated with preparation for subsequent agricultural season. In addition, drainage facilities will lead to reduced ET_a (large evaporation component) during the early months of irrigation season, ultimately resulting in improved water productivity.

83. The remote sensing based ET_a, AGBP and WP assessment indicates that large areas of all four irrigation schemes are currently dysfunctional owing to inadequate irrigation water supply to different sections of the command area. The estimated AGBP values in these systems were lower than the values estimated in other paddy dominant schemes. The derived water productivity estimates in these schemes must be used with caution and do not directly relate to the productivity of a rice-based system.

84. Since the SCIS, PPIS and C15IS are in the floodplains of the Mekong River, water availability to satisfy crop water consumption may not be a major issue considering their relatively small size. Rather, problems exist in inadequate irrigation infrastructure and water delivery from the source to different sections of the irrigation schemes.

V. LIST OF REFERENCES

Bastiaanssen, W.G.M., Menenti, M., Feddes, R.A., Holtslag, A.A.M., 1998a. A remote sensing surface energy balance algorithm for land (SEBAL). 1. Formulation. J. Hydrol. 212–213, 198–212.

Bastiaanssen, W.G.M., Pelgrum, H., Wang, J., Ma, Y., Moreno, J.F., Roerink, G.J., van der Wal, T., 1998b. A remote sensing surface energy balance algorithm for land (SEBAL).: Part 2: Validation. J. Hydrol. 212–213, 213–229.

Blatchford, M.L., Karimi, P., Bastiaanssen, W.G.M., Nouri, H., 2018. From global goals to local gains—a framework for crop water productivity. ISPRS Int. J. Geo-Inf. 7.

Cai, X., Thenkabail, P.S., Biradar, C.M., Platonov, A., Dheeravath, V., Cohen, Y., Goldlshleger, N., Ben Dor, E., Alchanatis, V., Vithanage, J., Markandu, A., Gumma, M., 2009. Water productivity mapping using remote sensing data of various resolutions to support “more crop per drop.” J. Appl. Remote Sens. 3, 033557-033557–23.

Cleveland, W.S., Devlin, S.J., 1988. Locally Weighted Regression: An Approach to Regression Analysis by Local Fitting. J. Am. Stat. Assoc. 83, 596–610.

Funk, C., Peterson, P., Landsfeld, M. Pedreros, D., Verdin, J., Shukla, S., Husak, G., Rowland, J., Harrison, L., Hoell, A., Michaelsen, J., 2015 The climate hazards infrared precipitation with stations—a new environmental record for monitoring extremes. Sci Data 2, 150066. https://doi.org/10.1038/sdata.2015.66

Irrigated Agriculture Improvement Project Stung Chinit Subproject Feasibility Report (IAIP)., 2019a. Cambodia: Irrigated Agriculture Improvement Project Project Stung Chinit Subproject, Feasibility study report. https://www.adb.org/sites/default/files/linked-documents/51159-002-sd-04.pdf

Irrigated Agriculture Improvement Project Prek Po Subproject Feasibility Report (IAIP)., 2019b. Cambodia: Irrigated Agriculture Improvement Project Project Prek Po Subproject, Feasibility study report. https://www.adb.org/sites/default/files/linked-documents/51159-002-sd-02.pdf

Irrigated Agriculture Improvement Project Canal 15 Subproject Feasibility Report (IAIP)., 2019c. Cambodia: Irrigated Agriculture Improvement Project Canal 15 Subproject, Feasibility study report. https://www.adb.org/sites/default/files/linked-documents/51159-002-sd-03.pdf

Jaafar, H.H., Ahmad, F.A., 2020. Time series trends of Landsat-based ET using automated calibration in METRIC and SEBAL: The Bekaa Valley, Lebanon. Remote Sens. Environ., Time Series Analysis with High Spatial Resolution Imagery 238, 111034.

Karimi, P., Bastiaanssen, W.G.M., 2015. Spatial evapotranspiration, rainfall and land use data in water accounting – Part 1: Review of the accuracy of the remote sensing data. Hydrol Earth Syst Sci 19, 507–532.

MAFF (2011). Annual Report 2010, Ministry of Agriculture, Fisheries and Forestry (MAFF), Phnom Penh, Cambodia.

Mainuddin, M., Kirby, M. 2009. Spatial and Temporal Trends of Water Productivity in the Lower Mekong River Basin, Agricultural Water Management 96 (11): 1567–1578

Metz, M., Andreo, V., Neteler, M., 2017. A New Fully Gap-Free Time Series of Land Surface Temperature from MODIS LST Data. Remote Sens. 9, 1333.

Mul, M., Karimi, P., Coerver, H.M., Pareeth, S., Rebelo, L.M., 2020. Water Productivity and Water Accounting Methodology Manual. Project report, IHE Delft Institute for Water Education, The Netherlands and the International Water Management Institute, Sri Lanka.

Neteler, M., 2010. Estimating Daily Land Surface Temperatures in Mountainous Environments by Reconstructed MODIS LST Data. Remote Sens. 2, 333–351.

Steduto, P., Hsiao, T.C., Fereres, E., Raes, D. (Eds.), 2012. In: FAO Irrigation and Drainage Paper Nr. 66. FAO, Rome, Italy

Tomar, V.S., O'Toole, J.C. 1980. Water use in lowland rice cultivation in Asia: A review of evapotranspiration. Agricultural Water Management, 1980, vol. 3, issue 2, 83-106